

A FIELD TRIP GUIDE FOR MARATHON OIL COMPANY

**STRUCTURAL EVOLUTION OF THE LEWIS THRUST SYSTEM IN GLACIER
NATIONAL PARK, WESTERN MONTANA**

AN YIN

Department of Earth and Space Sciences, University of California, Los Angeles, California 90024

May, 1993

FIELD TRIP OBJECTIVES

The purpose of the field trip is to show the style of deformation and cross-cutting relationships in the classic Lewis thrust system, Glacier National Park, western Montana. With the aid of detailed geologic maps and cross-sections, kinematic development of duplexes, imbricates, extensional faults, fault-bend/propagation folds and out-of-sequence thrusts in the Lewis thrust system is illustrated. In addition, the relationship between thrust kinematics and cross-section balancing is discussed. The field trip guide consists of two parts: (1) an overview of the Lewis thrust system in Glacier National Park and its evolutionary history, and (2) descriptions of field stops.

PART I: OVERVIEW OF THE LEWIS THRUST SYSTEM

INTRODUCTION

The Cordilleran foreland fold-and-thrust belt in the southern Canadian Rocky Mountains and northwestern Montana consists of two tectonic elements (Fig. 1): (1) an eastern imbricate-thrust belt, and (2) a western broad-fold belt. Understanding the structural origin of the broad-fold belt is important, because it is situated between a coeval magmatic belt to the west and the imbricate-thrust belt to the east. The magmatic and imbricate-thrust belts were speculated to have been related during their development (Burchfiel and Davis, 1975; Price, 1981). Debates have been centered on whether or not the crust below the broad-fold belt was significantly thickened during the overall development of the fold-and-thrust belt. Two models may explain the geometry of the broad folds: (1) the folds represent minor crustal shortening as expressed by their long wavelengths and low amplitudes, and (2) the folds were related to thrusting at a deeper crustal level and were the result of significant crustal shortening by the development of duplexes and fault-bend/propagation folds (Price, 1981; Cowan and Potter, 1986; Yoos et al., 1991; Yin and Kelty, 1991a).

The Lewis thrust, first recognized by Willis (1902), is one of the major structural components developed during the Late Cretaceous to early Tertiary in the foreland fold and thrust belt of the southern Canadian Rockies (Bally et al., 1966; Price, 1981) and western Montana (Mudge and Earhart, 1980). It bounds the broad-fold belt to the east and the imbricate-thrust belt to west. The fault can be traced along strike from Steamboat Mountain in west-central Montana (Mudge and Earhart, 1980) to the Rundle Range in southwestern Alberta, Canada (Dahlstrom et al., 1962; Fig. 2) for at least 450 km. A significant amount of shortening in this part of the Cordilleran foreland fold and thrust belt was accommodated along this single intracontinental thrust. In Glacier Park near the international boundary, the Lewis thrust juxtaposes the Middle Proterozoic Belt-Purcell Supergroup in its hanging wall over Cretaceous sedimentary rocks in its footwall, and displaces the Belt-Purcell rocks for at least 60 km to the northeast with respect to its footwall rocks (Price, 1962).

The first-order structural configuration of the Lewis plate has long been treated as a simple syncline, the Akamina syncline (Dahlstrom, 1970) that extends from North Kootenay Pass of southeastern British Columbia to Marias Pass of northwestern Montana (Ross 1959, Gordy and others, 1977). The Syncline is part of the broad-fold belt between the imbricate-thrust belt and the magmatic belt in western Montana. Recent studies of the Lewis thrust system in Glacier National Park, however, reveal that complex structures including duplexes, thrust-related fault-bend/propagation folds, conjugate contraction faults, and extensional faults lie underneath the little deformed Akamina syncline (Davis and Jardine, 1984; Yin et al., 1989; Hudec and Davis, 1989; Yin, 1991; Yin and Kelty, 1991a, 1991b; Yin and Oertel, 1993). In particular, formation of the Akamina syncline could have been related to development of duplexes and fault-bend/propagation folds in the Lewis thrust sheet (Yin and Kelty, 1991a; Yin and Oertel, 1993).

STRATIGRAPHY

Hanging-Wall Stratigraphy

The Belt-Purcell Supergroup in the Lewis thrust sheet consists of the Altyn, Appekunny, Grinnell, Empire, Helena, Snowslip, Shepard, Mount Shields, Bonner Quartzite, and McNamara Formations (Fig. 3a; see Whipple et al., 1984, for detailed descriptions). The Mount Shields Formation, Bonner Quartzite and McNamara Formation of the upper Belt-Purcell Supergroup are only preserved in the hanging wall of the Blacktail fault, an Eocene-Oligocene normal fault that is equivalent to the Flathead normal fault in Canada (Constenius, 1982; Bally et al., 1966). Correlation of the Belt and Purcell Supergroups in Glacier National Park, Whitefish Range, and adjacent parts of Canada is shown in Fig. 3b. Stratigraphy of the lower and middle Belt Supergroup in southern Glacier National Park is shown in Fig. 3c.

The Altyn Formation, lying along the base of the Lewis thrust sheet, consists of dolomite, dolomitic limestone, sandy dolomite, and quartz arenite. It is overlain disconformably by the Appekunny Formation, and is cut by the Lewis thrust below. The stratigraphy of the Altyn Formation is complicated by widespread intraformational bedding-subparallel faults such as the Scenic Point fault near Two Medicine Lake in southeastern Glacier National Park.

The Appekunny Formation comprises mostly argillite and minor quartz arenite. In eastern Glacier National Park, five laterally persistent quartz-arenite units in the formation are designated marker bed A through marker bed E. Using the tops of marker bed C, D, and E as boundaries, the Appekunny Formation is divided into four informal members. Similar to the Altyn Formation, the stratigraphy of the Appekunny Formation is complicated by a bedding-parallel fault, the Brave Dog fault that lies in member 3. This fault locally cuts downsection gently to the east (Yin et al., 1989), exhibiting a geometry of either an extensional fault or an out-of-sequence thrust.

The Grinnell Formation is composed mainly of thinly-bedded red argillite above the fault and red quartz arenite and thickly-bedded argillite below the fault. The stratigraphy of this formation is again complicated by a bedding-parallel fault, the Rockwell fault. The Empire Formation consists of interbedded quartz arenite, argillite, and minor limestone, and the Helena Formation comprises almost entirely of limestone. The Snowslip Formation consists of siltite, argillite, oolitic arenite, and pink quartz arenite. Resting on top of the Snowslip Formation is the

Shepard Formation that is composed mainly of carbonate rocks with minor thinly bedded quartz arenite. Its lithology closely resembles rocks of the Altyn and Helena Formations.

The Bonner Quartzite and the McNamara Formation are only exposed in the Mt. Shield area in the southwestern part of the park. The Bonner Quartzite consists dominantly of pinkish-gray to pale-red, very fine- to medium-grained feldspathic arenite and less amounts of interbedded siltite and dark-red argillite. The McNamara Formation is composed of green siltite, argillite, and calcareous arenite and quartz arenite. Its top is not preserved in the Park.

Footwall Stratigraphy

Stratigraphic units in the footwall of the Lewis thrust are exposed along the southern and eastern margins of Glacier National Park. They are described by Mudge and Earhart (1983) in detail. Briefly, these units include the Lower Cretaceous Kootenai Formation (nonmarine, grey-green and maroon mudstone), the Lower Cretaceous Blackleaf Formation (marine, grey mudstone and interbedded sandstone), and the Upper Cretaceous Marias River Shale (marine, dark-grey mudstone).

Kishenehn Formation

The Oligocene Kishenehn Formation (Constenius, 1982) was deposited in the hanging wall of the Blacktail/Flathead normal fault during its movement. It is at least 3,500 m thick and consists of light-grey to grey beds of sandstone, siltstone, mudstone in its lower part, and brick-red to brown-red mudstone, sandstone, and conglomerate in its upper part.

GEOMETRY AND KINEMATICS OF THE LEWIS THRUST SYSTEM

The structural framework of the Lewis thrust system in Glacier Park is schematically shown in Fig. 4. Detailed geologic mapping in Glacier National Park, Montana, reveals four episodes of deformation in the hanging wall of the Lewis thrust.

Pre-Lewis Thrust Structures

Pre-Lewis thrust structures consist of (1) the frontal zone that is characterized by west- and east-dipping imbricate thrusts, conjugate contraction faults, and west- and east-directed bedding-

parallel faults, and (2) the Scenic Point complex (Fig. 4). These structures are exposed along the eastern edge of the Lewis thrust sheet. Although they are truncated from below by the Lewis thrust (Figs. 5 and 6), their development was kinematically compatible with the emplacement of the Lewis thrust sheet. Thus, they predate the Lewis thrust and may have formed during early stages of the emplacement of the Lewis plate along thrust surfaces that lie below the present Lewis thrust. The extreme structural complexity of the frontal zone may have been related to the presence of a footwall ramp or a hanging-wall cutoff. Kinematic evolution of the frontal zone is shown in Fig. 7. Detailed descriptions of the frontal-zone structures are presented by Yin (1991).

The Scenic Point structural complex is shown in a cross-section in Fig. 8. It is constructed from both photos and field observations. It is a duplex, because it consists of steeply dipping minor thrusts that are bounded above and below by flat faults (Dahlstrom, 1970). Note that strata in the duplex is cut from top by an out-of-sequence roof fault. The Scenic Point complex is cut by faults of the frontal zone, and thus, it predates the Lewis thrust.

Two models have been proposed by Boyer and Elliott (1982) for the development of duplexes (Figs. 9a and 9b). The observed structural relationship in the Scenic Point complex resembles the duplex geometry produced by the kinematic history shown in Fig. 9b. Note that cross-sections such as those shown in Fig. 8 are difficult to balance if the offset strata in the hanging wall of the roof fault are not preserved, because mass is not conserved and the amount of the lost mass is hard to estimate.

Syn-Lewis Thrust Structures

Syn-Lewis thrust structures include (1) the late Cretaceous-early Tertiary Lewis thrust, (2) west-dipping Brave Dog and Rising Wolf duplexes, (3) east-dipping normal faults, (4) Mt. Walton fault-bend/propagation fold complex, and (5) the Akamina syncline (Fig. 4). The Akamina syncline is a broad fold that lies directly west of the Lewis thrust and extends northwestward for about 120 km from southern Glacier National Park, western Montana, to southeastern British Columbia and southwestern Alberta, Canada.

The Brave Dog and Rising Wolf duplexes are best exposed in southern Glacier National Park (Figs. 10). The geometry of the two duplexes differ from that proposed by Boyer and Elliott (1982; Fig. 9a), because the observed roof and floor thrusts in the Lewis thrust sheet (i.e., the Brave Dog, Rockwell, and Lewis thrusts) do not joint each other immediately on both sides of the duplexes cores as they suggested. In addition, the slip distribution along the roof faults of the duplexes in the Lewis thrust sheet is also different from the Boyer and Elliott model in that the magnitude of slip along the Brave Dog and Rockwell faults (9.0 km and 6.5 km, respectively; see Yin et al., 1989 and Yin and Kelty, 1991a for details) are much greater than the amount of shortening accommodated by the imbricate thrusts in the cores of the Brave Dog and Rising Wolf duplex systems (about 3.5 to 4 km). In Boyer and Elliott's model, the development of duplex systems is considered to be a slip-transfer mechanism from the floor thrust to the roof thrust, and thus, the magnitude of slip along the floor and roof thrusts and the amount of shortening absorbed by the imbricates in the core of the duplex should be equal.

During the development of a thrust system, the crustal section may undergo simple shear, pure shear, or a combination of both. Experimental rock mechanics show that pure-shear deformation results in a conjugate set of faults whereas simple-shear deformation results in the formation of Riedel and primary shears (Fig. 11; see Yin and Kelty, 1991b for references). On the basis of this mechanical concept and the observation that bedding-parallel simple shear is the dominant mode of deformation in the Lewis thrust sheet in Glacier National Park, Yin et al. (1989) propose that the development of the Brave Dog and Rising Wolf duplexes is a result of simple-shear deformation (Fig. 12). In particular, the imbricate thrusts in the cores of the two duplexes were developed as primary shears in a simple-shear system. The widespread east-dipping normal faults in the Park were also explained as a consequence of simple-shear deformation (Fig. 13; Yin and Kelty, 1991b).

A fault-bend/propagation fold complex is exposed in western-central Glacier National Park (Fig. 14). It is described in details by Yin and Oertel (1993). The complex involves rocks of the upper Grinnell Formation, the Empire Formation, and the Helena Formation. This complex

consists of the Gunsight thrust at its base (Fig. 15a), an east-verging fault bend/propagation fold above the Gunsight thrust (Fig. 15a), a frontal fold complex (Fig. 15b), and a west-directed roof thrust, the Mt. Thompson fault, on the top of the frontal fold complex (Fig. 15c).

The cut-off angle between the Gunsight thrust and bedding in its footwall is about 70° . Bedding of the steep forelimb of the fault-bend/propagation fold is truncated by the Gunsight thrust below. The cut-off angle ranges from 70° to 90° . The fold interlimb angle of the anticline is about 120° in the northern part of the area and about 90° in the southern part.

Both limbs of the hanging wall anticline are complexly deformed. Deformation in the forelimb is characterized by W-directed thrusts with offsets of less than 20 m and minor folds. The shallow-dipping backlimb is deformed by a few E-verging overturned folds. The total bedding-parallel shortening strain of the forelimb by thrusting, folding, and penetrative strain is no more than 20%, because no significant change in stratigraphic thickness across the hinge of the hanging wall anticline can be detected in the field.

The 4-km wide west-verging fold belt (Fig. 14) is bounded above by the Mt. Thompson fault, which lies in the lower part of the Helena Formation between dominantly limestone above and interbedded limestone and quartz arenite below. Minor W-verging folds with both amplitudes and wavelengths of several meters are present directly below the Mount Thompson fault, suggesting that it is W-directed. The Mount Thompson fault is different from the "passive roof fault" of Banks and Warburton (1986), because nowhere in the study area is it directly linked with the Gunsight fault to form the tipline of a blind thrust (cf. fig. 7 of Banks and Warburton, 1986). It is merely an accommodation zone or decollement separating the highly folded strata below from less folded strata above. For the same reason, the frontal fold complex does not resemble a "triangular zone" of Price (1986).

The E-verging hanging wall anticline above the Gunsight thrust exhibits the geometry of a fault-bend fold (Rich, 1934). It could thus have developed according to the kinematic model of Suppe (1983). However, when the model is applied assuming constant bed thickness during folding (eq. 12, Suppe, 1983) and using the observed initial cut-off angle (70°), the predicted

interlimb angle ($2g$) of the anticline and the final cut-off angle (b) are 176° and 8° for the mode I fold and 20° and 160° for the mode II fold. However, the observed interlimb and final cut-off angles, $2g = 90\text{-}120^\circ$ and $b = 70\text{-}90^\circ$, are both inconsistent with the model. Considering uniform forelimb thickening and applying Jamison's fault-bend fold model (fig. 3 of Jamison, 1987), no solution exists for observed interlimb angles of $90\text{-}120^\circ$ and an initial cut-off angle of 7° , no matter how much forelimb thickening one assumes. It is, however, conceivable that the fold originated from an initial, open mode I fault-bend fold, and that the observed interlimb angle of $90\text{-}120^\circ$ resulted from later tightening of the fold. Alternatively, the thrust ramp could have been initiated as a steeper surface and later became shallow due to a simple-shear deformation in its footwall that flattens the ramp; this process can also lead to the observed fold geometry (Fig. 16).

An apparent Rich-type fault-bend fold (Rich, 1934) can also be the result of fault-propagation folding because the two types of fold share many geometric features (Jamison, 1987; Suppe and Medwedeff, 1990; Mitra, 1990). However, applying Jamison's fault-propagation model (Fig. 2 of Jamison, 1987) together with forelimb thickening, we again found no solution for the observed interlimb angles of $90\text{-}120^\circ$ starting from an initial cut-off angle of 7° . With 20% forelimb thickening strain the predicted fold interlimb angle is about 10° , much tighter than observed. It seems unlikely that the observed angle of $90\text{-}120^\circ$ resulted from reopening a tight fold from an initial interlimb angle of 10° , because, contrary to observations, this would require flexural W-verging folding and thrusting in the backlimb and E-verging features in the forelimb.

The poor fit of the observed geometry with all constant-volume balanced cross-section models could be due to significant volume loss during or after folding. The widespread spaced cleavage could well have been the result of volume loss by stress solution.

It should also be noted that the geometry of the entire thrust-related fold complex in west-central Glacier National Park differs from either a fault-bend fold or a fault-propagation fold by possessing (1) a passive roof fault that transports in the direction opposite to that of the basal thrust, (2) a complexly deformed fold zone in front of an asymmetric hanging wall anticline

between the basal thrust and the roof fault, and (3) an over-gentler thrust ramp. The development of the Mt. Thompson roof fault caused the disharmony of folding above and below.

The structural relations discussed above provide the basis for a kinematic model that explains the development of the fault-bend/propagation fold complex (Fig. 17). Emplacement of the Lewis thrust sheet started with the initiation and development of the Brave Dog duplex between the Lewis and the antiformal Brave Dog faults (Figs. 17a and 17b). The development of the Brave Dog fault was followed by the initiation, above it, of the Gunsight thrust in the anticlinal Grinnell Formation (Fig. 17b). We speculate that the Gunsight thrust ramp was localized by the presence of the anticline, produced in turn by the Brave Dog duplex. Because this is a gentle warp of only a few degrees on either limb, less energy may have been expended by the Gunsight thrust following the curved bedding plane than would have been needed to cut bedding along a new, straight fault segment. The E-verging hanging wall anticline above the Gunsight fault could have been initiated as an open fault-bend fold (Fig. 17c). Further emplacement of the Gunsight plate caused both the development of the frontal fold complex and the tightening of the hanging wall anticline (Fig. 17d). Associated with the latter are the development of E-directed flat faults in the backlimb and W-directed thrusts in the forelimb. The backlimb was stretched as it passed the thrust ramp. The top-to-the-west bedding-parallel Mt. Thompson fault was initiated as a consequence of the piling up of the frontal fold complex (Fig. 17d). Further fold tightening in this complex led to the formation of the cleavage S₁ in hinge zones (Fig. 17d). During or after the emplacement of the Gunsight thrust sheet the regional, west-dipping cleavage S₂ developed (Fig. 17e).

The formation of the segment of the Akamina syncline in the study area was the consequence of development of the duplexes and fault-bend/propagation folds in the Lewis thrust sheet, because strata above the duplexes and thrust-related folds are concordant with the syncline. The syncline is, however, discordant with the Lewis thrust, because the Lewis thrust in southern Glacier National Park is hardly folded (Fig. 18). This observation contrasts strongly with the well-established concordant relationship between the Lewis thrust and the Akamina syncline in its hanging wall in Canada, about 100 km north of the study area (Fig. 19).

We propose a deformation history for this part of the Lewis plate based on crosscutting relationships outlined above (Fig. 20). The chronological order for the formation of major structural elements is: (1) the Scenic Point structural complex, (2) the frontal zone, (3) the Lewis thrust, (4) the Brave Dog Mountain duplex and east-dipping normal fault system, (5) the Rising Wolf Mountain duplex, and (6) the Akamina syncline.

During the initial stages of development of the Scenic Point structural complex (Figs. 20a to c), imbricate thrust faults branched off from an older basal thrust located structurally below the present Lewis thrust. These imbricates were later cut and offset by the Scenic Point fault above. This event was followed by development of the frontal zone (Figs. 20c to f). Field relationships in the frontal zone (Yin, 1991) suggest that thrusts developed along two bedding-parallel decollements, one along the Altyn-Appekunny contact and one in the Altyn Formation (Figs. 20c and d). We assume in Figure 20d that the deeper decollement of the frontal zone shares the same sole fault as the Scenic Point complex.

Rotation of structures in the eastern part of the frontal zone (Fig. 20e) is inferred to explain the apparent west-dipping normal faults (Yin, 1991). The rotation may predate the formation of conjugate contraction faults in the western frontal zone, because they were not rotated (Fig. 20f).

After the formation of the frontal zone, the speculated pre-Lewis basal thrust and the Scenic Point fault were gently folded. Structures in the frontal zone and the Scenic Point complex were later cut and offset by the Lewis thrust that lies structurally higher than the early basal fault (Figs. 20f and g).

Following the formation of the Lewis thrust, the Brave Dog fault began to propagate parallel or subparallel to bedding in the Appekunny Formation (Figs. 20g and h). Its initiation may have been related to east-verging simple-shear deformation produced by eastward movement along the Lewis thrust (Yin et al., 1989). The Brave Dog fault, which cuts structures in the underlying frontal zone, became kinematically linked with the Lewis thrust through the Elk Mountain imbricate system. The Brave Dog fault was broadly warped upward over the imbricate system as a geometric consequence of shortening across the imbricate system (Fig. 20h). During movement of

the Brave Dog fault and simultaneous movement along the Lewis thrust, the east-dipping normal fault system developed as a consequence of simple-shear deformation between the two faults (Yin and Kelty, 1991b).

The Rockwell fault was initiated at a higher structural level above the Brave Dog fault and propagated subparallel to bedding in the Grinnell Formation (Figs. 20h and 20i). The Rockwell fault later became kinematically linked with the Lewis thrust through the development of the Mount Henry imbricate system along the east side of the study area. The development of the imbricate system beneath the Rockwell fault caused the upward warping of the low-angle fault. Development of the Rising Wolf Mountain and the Brave Dog Mountain duplexes, together, resulted in formation of the Akamina syncline that is defined by strata above the Rockwell fault (Fig. 20i).

Two models have been proposed for the formation of the Akamina syncline: (1) the formation of the syncline was related to movement along the Flathead (or Blacktail) normal fault (Dahlstrom, 1970), and (2) the formation of the syncline was related to duplex formation and imbricate thrusting in the footwall of the Lewis thrust (Bally et al., 1966; Gordy et al., 1977). The result of this study suggests that neither model explains the structural relationship observed in southern Glacier National Park. First, although the short-wavelength antiforms and synforms of the Lewis thrust close to the Blacktail normal fault may have been related to movement along this younger fault, the overall geometry of the long-wavelength Akamina syncline is compatible with the development of the duplexes and the fault-bend/propagation fold in the *hanging wall* of the Lewis thrust (Fig. 20h). Second, imbricate thrusting in the Mesozoic and Paleozoic strata in the footwall of the Lewis thrust may have affected the geometry of the Lewis thrust in the south-central part of the study area. The resultant geometry (a broad antiform) is, however, discordant with the Akamina syncline as discussed above. Thus, we conclude that at least in southern Glacier National Park the formation of the Akamina syncline was related to deformation in the hanging wall of the Lewis thrust during emplacement of the Lewis plate. This interpretation leads to a paradox in that the Lewis thrust is clearly folded into a synform in southwestern Alberta and

southeastern British Columbia, Canada, directly north of the international border as indicated by surface (presence of thrust windows) and subsurface (well and seismic) data (Bally et al., 1966; Dahlstrom, 1970; Gordy et al. 1977; Fig. 19).

To reconcile the discrepant observations on the geometry of the Lewis thrust north and south of the international border, we propose a model to explain the structural relationship between the Akamina syncline and deformation in the hanging wall and footwall of the Lewis thrust (Fig. 21). In this model, the development of the syncline was related to duplex formation and imbricate thrusting in two structural levels, one above and one below the Lewis thrust. The magnitude of shortening in the duplex and imbricate systems in the hanging wall and the footwall vary along the structural trend. The magnitude of NE-SW horizontal shortening decreases in the footwall and increases in the hanging wall southward. The total shortening of the hanging wall and footwall could be approximately uniform along the structural trend in the NW-SE direction. The role of the Lewis thrust was to transfer shortening *laterally* along the regional structural trend (NW-SE) from its footwall in the Paleozoic and Mesozoic strata to its hanging wall in the Proterozoic Belt strata. Although the deformation in the Lewis plate north of the international border is more complicated than what is shown in Figs. 19 and 21, the presence of thrust windows (Fig. 1) north of the international border requires that the Lewis thrust is significantly folded (Fermor and Price, 1987).

Post-Lewis Thrust Contractional Structures

Post-Lewis thrust contractional structures include the Lone Walker fault, a high-angle reverse fault that cuts the Lewis thrust and strikes N70°W, which is about 30-40° more westerly than the average strike of the syn-Lewis thrust structures. The development of this fault represents a change in compressional direction after emplacement of the Lewis plate.

Post-Lewis Thrust Extensional Structures

Post-Lewis thrust extensional structures include southwest-dipping normal faults. These faults are part of the Eocene-Oligocene Rocky Mountain trench normal fault system.

PART II: DESCRIPTIONS OF FIELD STOPS

STOP (1) Highway 2, ~4 miles west of East Glacier:

Overview of the geology of the Lewis thrust system. From this stop, we can see the Lewis thrust to the north that lies at the break of slope. It separates the Altyn Formation (light-yellow cliff-forming unit) in the hanging wall and the Cretaceous sedimentary rocks (poorly exposed, dark-grey slope-forming unit) in its footwall. We can also see the frontal-zone structures, the Mt. Henry imbricate thrusts which is part of the Rising Wolf duplex, and the Lone Walker reverse fault that offsets the Lewis thrust.

STOP (2) Highway 2, ~10 miles west of East Glacier:

Discussion on duplex development and abandonment during the evolution of the Lewis thrust system. Overview of mechanisms for the formation of extensional faults in thrust systems. View to the north is the Brave Dog fault that is cut by thrusts of the Mt. Henry imbricate system. Numerous east-dipping normal faults lie directly above the Lewis thrust (Fig. 22).

STOP (3) Highway 2, Marias Pass at the Continental Divide:

Overview of the geometry of the Lewis thrust surface and its relationship to duplex systems in its hanging wall and footwall. View to the northwest is Elk Mountains where the lower part of the Brave Dog duplex system is exposed (Fig. 23).

STOP (4) Two Medicine Lake, southeastern Glacier National Park:

Overview of the role of out-of-sequence in the development of duplex systems. If the lighting is right, we may see two antiformal-stack duplexes. They formed during multiple episodes of deformation such as development of multiple roof thrusts.

STOP (5) Jackson Glacier, Going-to-the-Sun Road:

Overview of the fault-bend/propagation fold complex developed in the Lewis thrust sheet in west-central Glacier National Park. A view southwards this point is the western steeply dipping limb of the hanging wall anticline in this thrust-related fold complex. This fold complex together with the Brave Dog duplex beneath it define the western limb of the broad Akamina syncline in the park.

STOP (6) On the International Highway northeast of Chief Mountain:

View to the west from the Chief Mountain International Highway is the Chief Mountain duplex (Fig. 24). Note that the roof thrust of the duplex cuts both bedding and thrusts in its footwall, exhibiting out-of-sequence thrust geometry. This is a classic outcrop of duplex structures. It was first described together with the Yellow Mountain duplex to the south by Willis (1902).

The Yellow Mountain duplex was investigated by Davis and Jardine (1984). Geologic map and cross-section of the Yellow Mountain duplex system ^{are} shown in Fig. 25.

REFERENCES CITED

- Bally, A. W., Gordy, P. L., and Stewart, G. A., 1966, Structure, seismic data, and orogenic evolution of southern Canadian Rockies: *Bulletin of Canadian Petroleum Geologists*, v. 14, p. 337-381.
- Boyer, S. E., and Elliott, D., 1982, Thrust systems: *American Association of Petroleum Geologists Bulletin*, v. 14, p. 337-381.
- Burchfiel, B. C., and Davis, G. A., 1975, Nature and controls of Cordilleran orogenesis, western United States: extensions of an earlier synthesis: *American Journal of Sciences*, v. 275, p. 363-396.
- Banks, C.J., and Warburton, J., 1986, "Passive roof" duplex geometry in the frontal structures of the Kirhar and Sulaiman mountain belt, Pakistan. *Journal of Structural Geology*, v. 8, p. 229-238.
- Constenius, K., 1982, Relationship between the Kishenehn Basin, and the Flathead listric normal fault system and the Lewis thrust salient, *in* Powers, R.B., ed., *Geologic Studies of the Cordilleran Thrust Belt*, Rocky Mountain Association of Geologists, p. 817-830.
- Cowan, D. S., and Potter, C. J., 1986, Continent-oceans transect B-3: Juan de Fuca spreading ridge to Montana thrust belt: Boulder, Colorado, Geological Society of America.
- Dahlstrom, C. D. A., Daniel, R. E., and Henderson, G. G. L., 1962, The Lewis thrust at Fording Mountain, British Columbia: *Alberta Society of Petroleum Geologists Journal*, v. 10, p. 373-395.
- Dahlstrom, C. D. A., 1970, Structural geology in the eastern margin of the Canadian Rocky Mountains: *Bulletin of Canadian Petroleum Geologists*, v. 18, p. 332-406.
- Davis, G. A., and Jardine, E. A. 1984. Preliminary studies of the geometry and kinematics of the Lewis allochthon, Saint Mary Lake to Yellow Mountain, Glacier National Park, Montana. *Montana Geol. Soc. 1984 Field Conf. Guidebook*, p. 201-209.
- Gordy, P. L., Frey, F. R., and Norris, D. K., 1977, Geological guide for the C.S.P.G. 1977 Waterton-Glacier Park field conference, Canadian Society of Petroleum Geologists, 93 pp.

- Harrison, J. E., Griggs, A. B., and Wells, J. D., 1974, Tectonic features of the Precambrian Belt Basin and their influence on post-Belt structures: U.S. Geological Survey Professional Paper 866, 15 pp.
- Harrison, J. E., Kleinfelt, M. D., and Wells, J. D., 1980, Phanerozoic thrusting in Proterozoic Belt rocks, northwestern United States: *Geology*, v. 8, p. 407-411.
- Harrison, J. E., Grigg, A. B., and Wells, J. D., 1986, Geologic and structural maps of the Wallace 1°x2° quadrangle, Montana and Idaho: U.S. Geological Survey miscellaneous investigations series map I-15609-A.
- Hudec, M. R., and Davis, G. A., 1989, Out-of-sequence thrust faulting and duplex formation in the Lewis thrust system, Spot Mountain, southeastern Glacier National Park, Montana: *Canadian Journal of Earth Sciences*, v. 26, p. 2356-2364.
- Jamison, W. R., 1987, Geometric analysis of fold development in overthrust terranes: *Journal of Structural Geology*, v. 9, p. 207-219.
- Jardine, E. A., 1985, Structural geology along a portion of the Lewis thrust fault [M.S. thesis]: Los Angeles, University of Southern California, 205 pp.
- Kelty, T. K., 1985, The structural geology of a portion of the Lewis thrust plate, Marias Pass, Glacier National Park, Montana [M.S. thesis]: Los Angeles, University of Southern California, 226 pp.
- Mitra, S., 1990, Fault-propagation folds: Geometry, kinematic evolution, and hydrocarbon traps: *American Association of Petroleum Geologists Bulletin*, v. 74, p. 921-945.
- Mudge, M. R., 1982, A resume of the structural geology of Northern Disturbed Belt, northwestern Montana: in Powers, R. B., ed., *Geologic Studies of the Cordilleran Thrust Belt*, Rocky Mountain Association of Geologists, p. 91-122.
- Mudge, M. R., and Earhart, R. L., 1980, The Lewis thrust fault and related structures in the disturbed belt, northwestern Montana: U.S. Geological Survey Professional Paper 1174, 18 pp.

- Mudge, M. R., and Earhart, R. L., 1983, Bedrock geologic map of part of the northern disturbed belt, Lewis and Clark, Teton, Pondera, Glacier, Flathead, Cascade, and Powell Counties, Montana: U. S. Geological Survey, Miscellaneous Investigations series, Map I-1375.
- Price, 1962, Fernie map area, east half: Alberta and British Columbia 82G, east half: Geological Survey of Canada Paper 61-24.
- Price, R. A., 1981, The Cordilleran foreland thrust and fold belt in the southern Canadian Rocky Mountains, *in* McClay, K. R., and Price, N. J., eds., *Thrust and Nappe Tectonics*, Geological Society of London Special Publication 9, p. 427-446.
- Price, R.A., 1986, The southeastern Canadian Cordillera; thrust faulting, tectonic wedging, and delamination of the lithosphere: *Journal of Structural Geology*, v. 8, p. 239-254.
- Rich, J. L., 1934, Mechanics of low-angle overthrust faulting as illustrated by Cumberland thrust block, Virginia, Kentucky, Tennessee: *American Association of Petroleum Geologists Bulletin*, v.18, p. 1584-1596.
- Ross, C. P., 1959, Geology of Glacier National Park and Flathead region, northwestern Montana. Prof. Pap. U.S. Geological Survey 296, p. 1-125.
- Suppe, J. 1983, Geometry and kinematics of fault-bend folding: *Am. J. Sci.*, v. 283, p. 684-721.
- Suppe, J., and Medwedeff, D. A., 1990, Geometry and kinematics of fault-propagation folding: *Ecolgae geol. Helv.*, v. 83, p. 409-454.
- Whipple, J. W., Connor, J. J., Raup, O. B., and McGimsey, R. G., 1984, Preliminary report on stratigraphy of the Belt Supergroup, Glacier National Park and adjacent Whitefish Range, Montana: Montana Geological Society, 1984 Field Conference, Guidebook, p. 33-50.
- Willis, B., 1902, Stratigraphy and structure, Lewis and Livingston ranges, Montana: *Geological Society of America Bulletin*, v. 13, p. 305-352.
- Yin, A., 1988, Structural geology of the Lewis allochthon in a transect from Head Mountain to Peril Peak, southern Glacier National Park, Montana [Ph.D. thesis]: Los Angeles, University of Southern California, 290 p.

- Yin, A., Kelty, T. K., and Davis, G. A., 1989, Duplex development and abandonment during the evolution of the Lewis thrust system: *Geology*, v. 17, p. 806-810.
- Yin, A., and Kelty, T.K., 1991a. Structural evolution of the Lewis plate in Glacier National Park, Montana: Implications for regional tectonic development: *Geological Society of America Bulletin*, v. 103, p. 1073-1089.
- Yin, A., and Kelty, T. K., 1991b, Development of normal faults during emplacement of a thrust sheet: an example from the Lewis allochthon, Glacier National Park, Montana: *Journal of Structural Geology*, v. 13, p. 37-47.
- Yin, A., 1991, Complex Pre-Lewis thrust deformation, southeastern Glacier Park, Montana: *Mountain Geologist*, v. 28, p. 91-103.
- Yin, A., and Oertel, G., 1993, Kinematics and strain distribution of a thrust-related fold system in the Lewis thrust plate, northwestern Montana (U.S.A.), *Journal of Structural Geology*, in press.
- Yoos, T. R., Potter, C. J., Thigpen, J. L., and Brown, L. D., 1991, The Cordilleran foreland thrust belt in northwestern Montana and northern Idaho from COCORP and industry seismic reflection data: *American Association of Petroleum Geologists*, v. 75, p. 1089-1106.

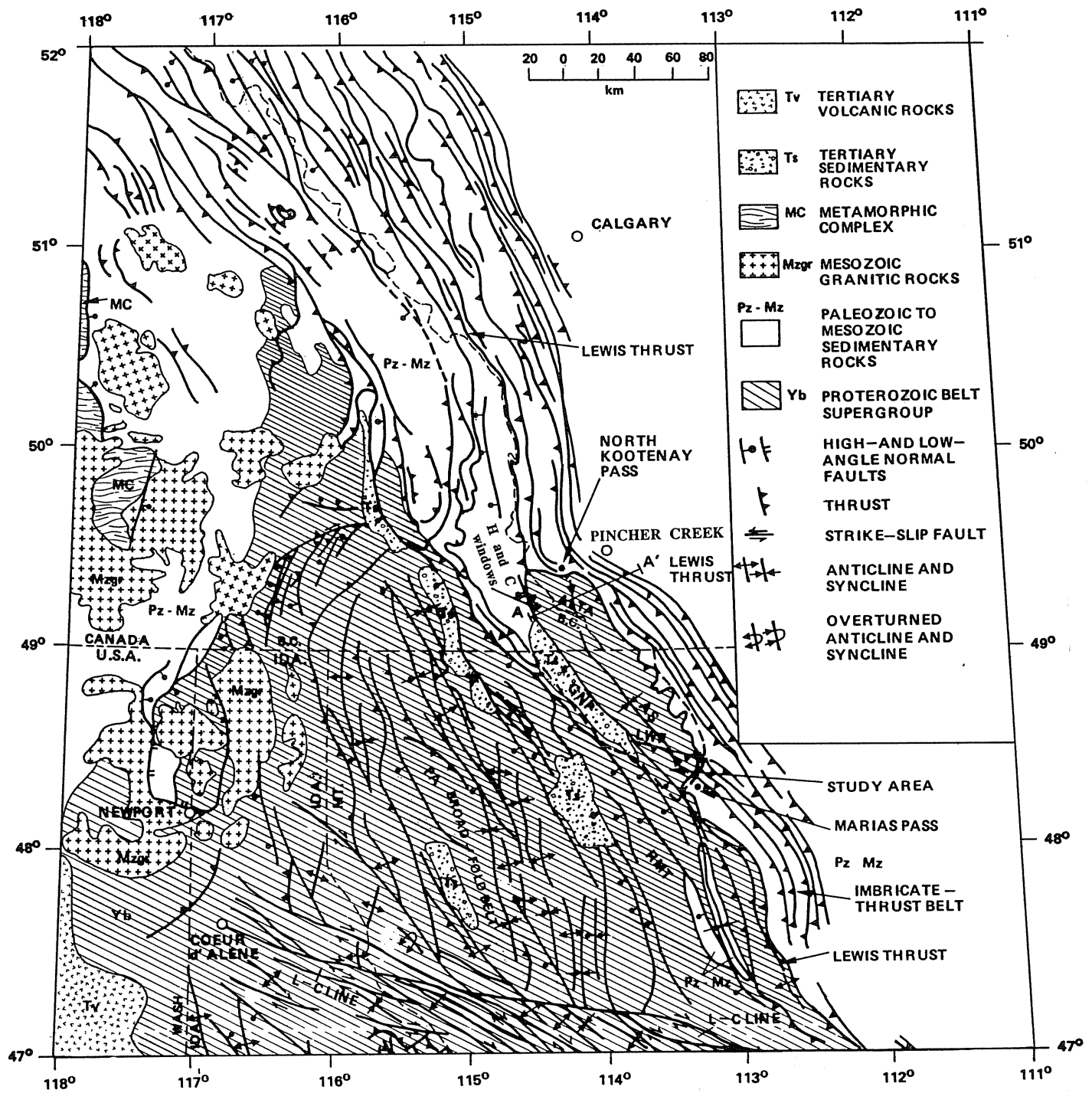


Fig. 1. Geologic map of Cordilleran foreland fold and thrust belt in southern Canadian Rocky Mountains and northwestern Montana between 47°N to 52°N latitude, after Bally et al. (1966), Dahlstrom (1970), Price (1981), Harrison et al. (1974, 1980; 1986), Mudge and Earhart (1980; 1983). Location of Glacier National Park (GNP, outlined by dashed line) and study area. Fold-and-thrust belt consists of two elements: (1) eastern imbricate-thrust belt which occurs mostly in Paleozoic and Mesozoic sedimentary rocks, and (2) a western broad-fold belt which occurs mostly in Proterozoic Belt Supergroup. Cross section A-A' shown in Fig. 19. AS, Akamina syncline; GNP, Glacier National Park; H and C windows, Haig Brook and Cate Creek windows; L-C line, Lewis-Clark line; LWF, Lone Walker fault (new name from this study); PA, Purcell anticlinorium; RMT, Eocene-Oligocene Rocky Mountain trench normal fault system.

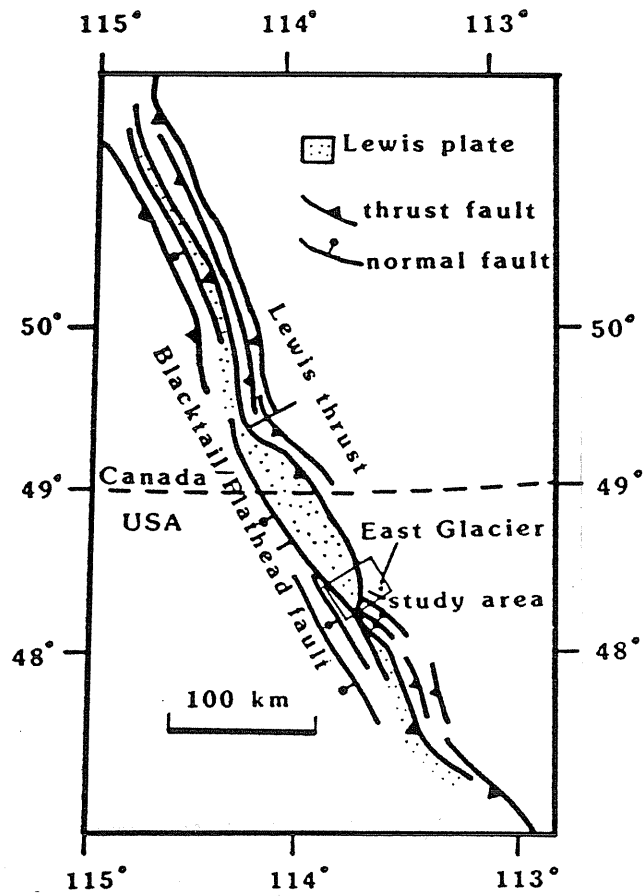


Fig. 2. Regional tectonic map of the Lewis thrust (after Yin et al., 1989).

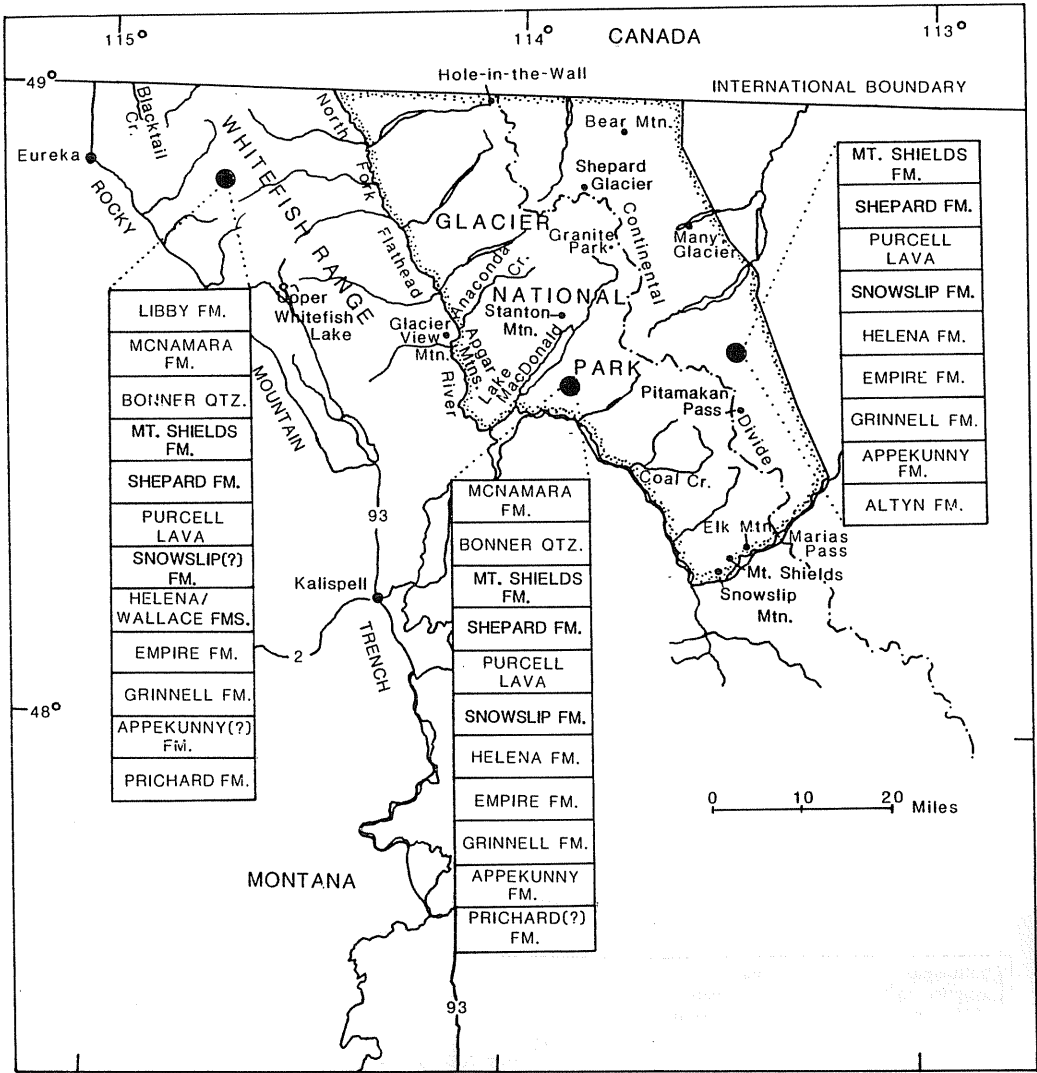


Fig. 3 a. Stratigraphic nomenclature of the Belt Supergroup in Glacier National Park; b. Stratigraphic correlation of the Belt and Purcell Supergroups in western Montana and adjacent parts of Canada; c. Stratigraphic section of the Belt Supergroup in southern Glacier Park.

WHITEFISH RANGE 1/			GLACIER NATIONAL PARK 1/				SOUTHEAST BRITISH COLUMBIA 2/				
			West		East						
Belt Supergroup	Missoula Group	Cambrian	Flathead Quartzite				Cambrian				
		Libby Formation	Top not exposed				Roosville Formation				
		McNamara Formation	McNamara Formation				Phillips Formation				
		Bonner Quartzite	Bonner Quartzite				Gateway Formation				
		Mount Shields Formation	5	Mount Shields Formation	5	Top not exposed		Upper member			
			4		4	Mount Shields Formation			Lower member		
			3		3	Lava					
			2		2						
			1		1						
		Shepard Formation	Shepard Formation		Shepard Formation		Sheppard Formation				
	Upper part	6	Purcell Lava	6	Purcell Lava	6	Nichol Creek Formation				
	Snowslip Formation	6	Snowslip Formation	5	Snowslip Formation	5	Van Creek Formation				
		4		4		4					
		3		3		3					
		2		2		2					
1		1		1							
Lower part 3/											
Middle Belt carbonate	Helena and Wallace Formations		Helena Formation		Helena Formation		Kitchener Formation				
Ravalli Group	Empire Formation		Empire Formation		Empire Formation		Upper member				
	Grinnell Formation 4/		Grinnell Formation 4/		Grinnell Formation 4/		Lower member				
	Appekunny(?) Formation		Appekunny Formation 4/	5	Appekunny Formation 4/	5	Creston Formation				
				4		4					
Lower Belt	Prichard Formation	Upper part	Prichard(?) Formation	Upper part	Altyn Formation					Aldridge Formation	
		Lower part	Lower part	Base not exposed							
	Base not exposed		Base not exposed		Base not exposed		Base not exposed				

Fig. 3b

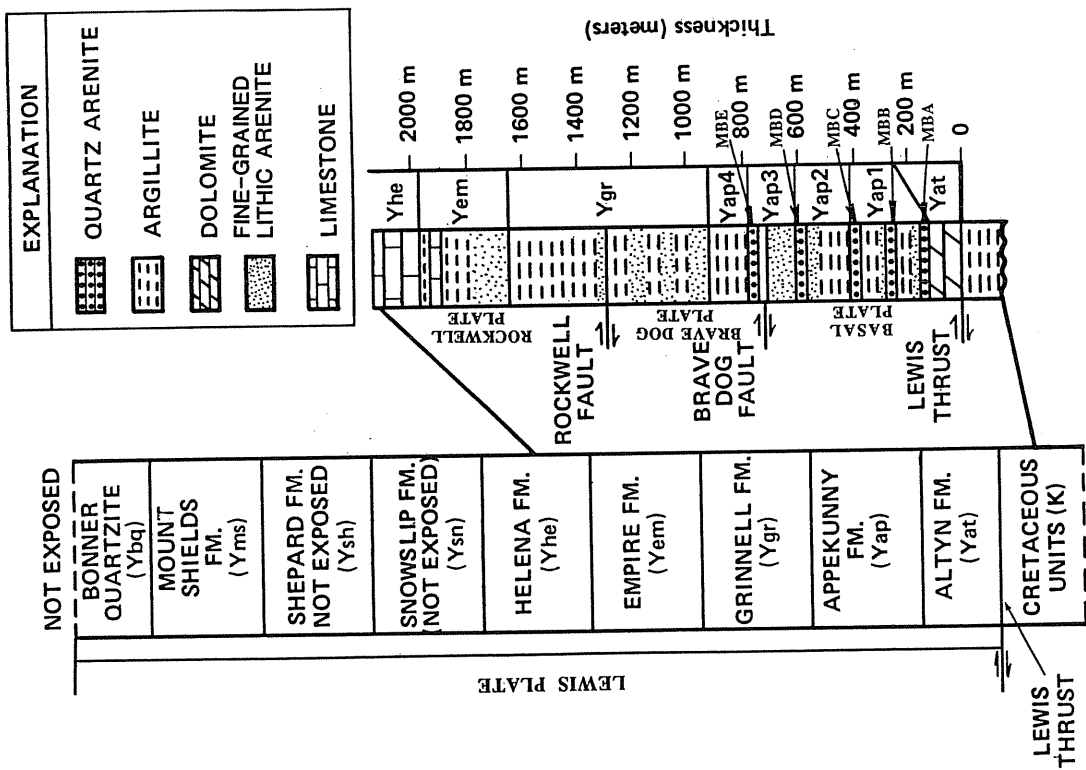


Fig. 3c

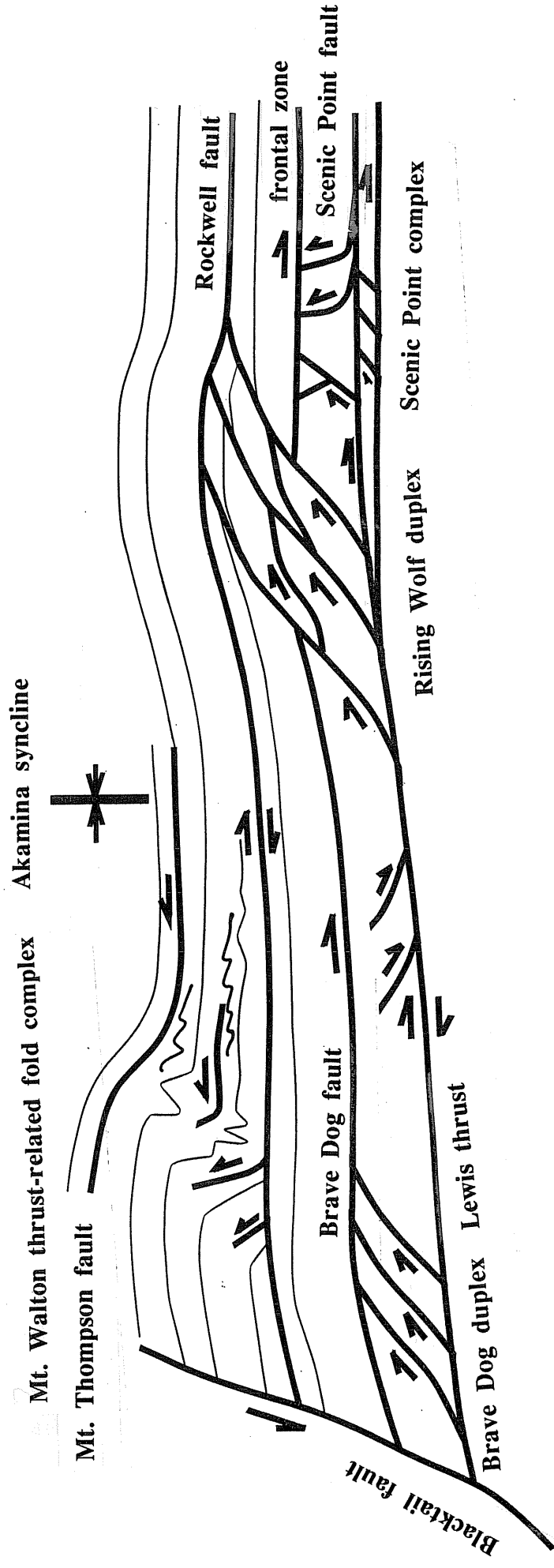


Fig. 4. Schematic cross-section of the Lewis thrust system in Glacier National Park.

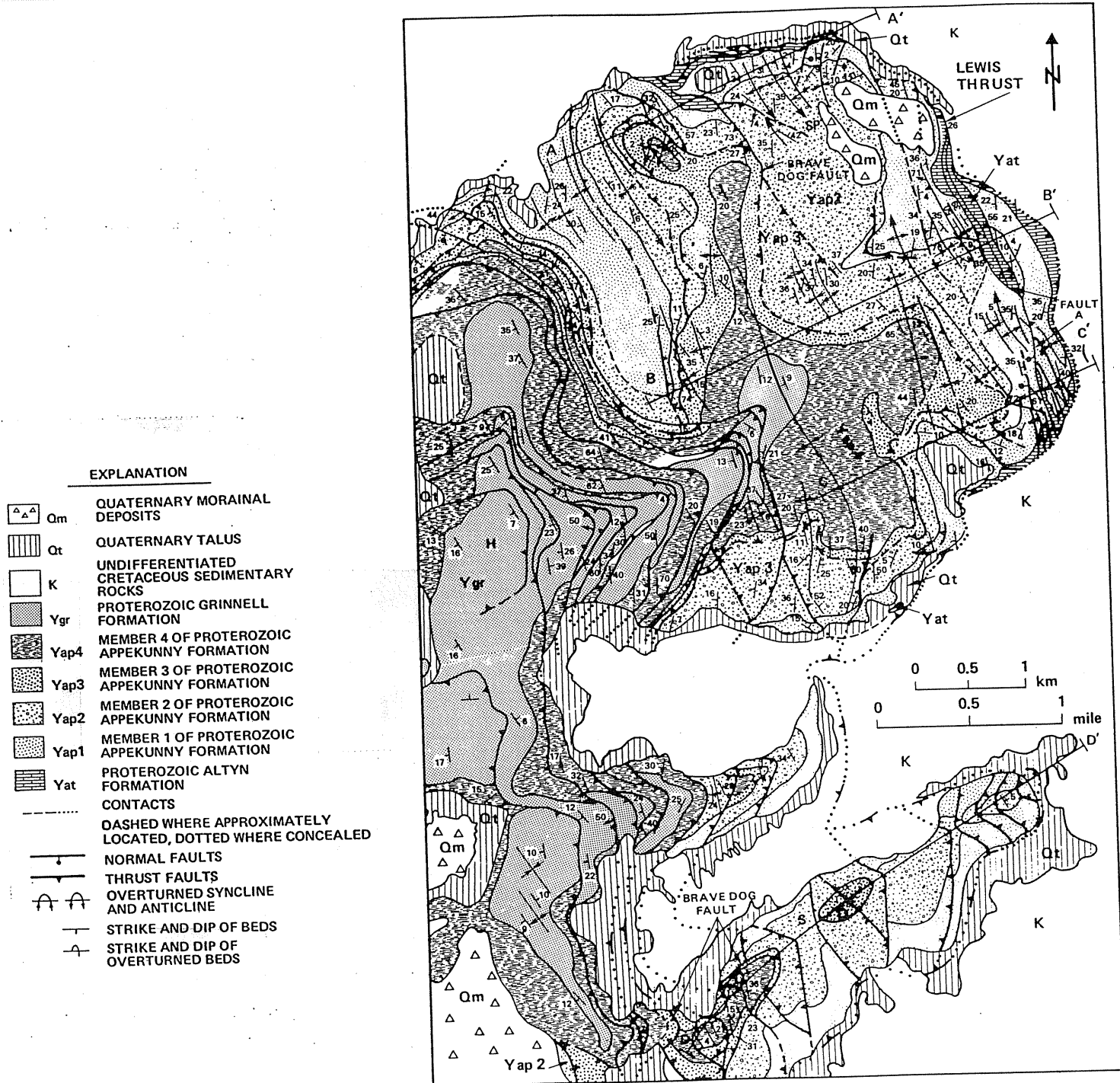


Fig. 5. a: Simplified geologic map of northeastern part of study area from Yin (1988) and locations of cross sections AA', BB', CC', and DD' shown in Figure 6b. Note fault A in frontal zone changes dip direction along its strike. The segment with west-dipping normal-fault geometry is interpreted to be result of locally east-verging rotation of primary east-dipping thrust. See Figure 2 for location of the map. H, Mount Henry; S, Squaw Mountain; SP, Scenic Point.

b: Geologic cross sections through lines AA', BB', CC', and DD'. Note that fault A dips to east in section BB' and west in section CC'. Faults in frontal zone cut Scenic Point structural complex; the complex is, in turn, cut by overlying Brave Dog fault. Absence of Scenic Point structural complex in section CC' is due to truncation by Lewis thrust. MHIS in cross section DD', imbricates in Rising Wolf Mountain duplex.

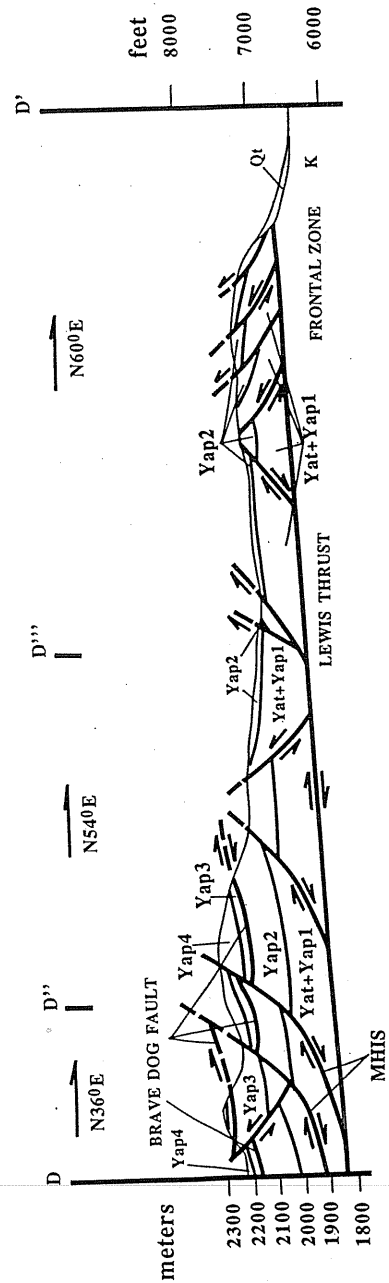
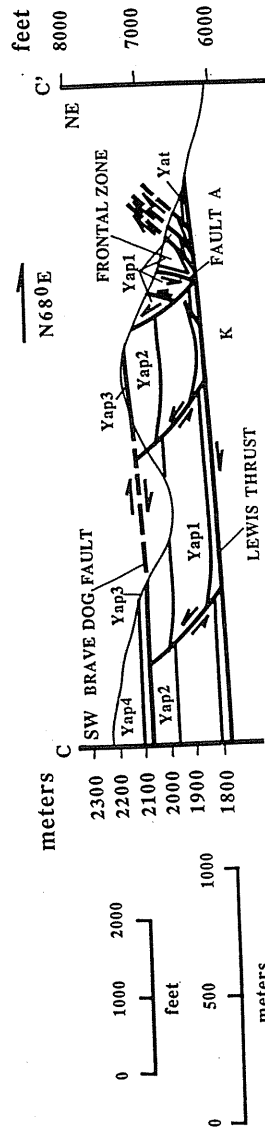
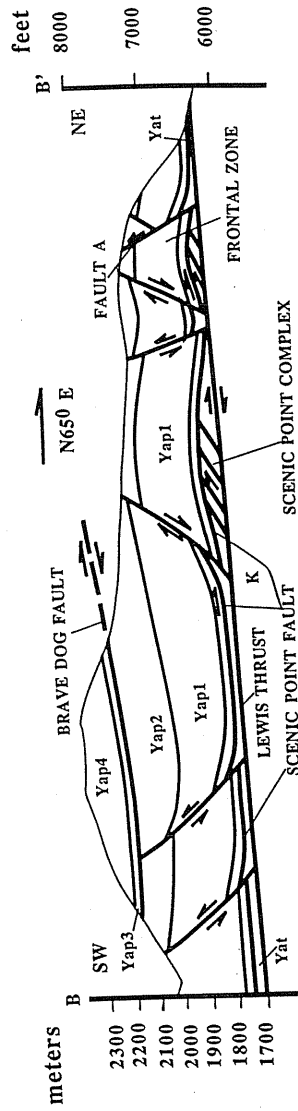
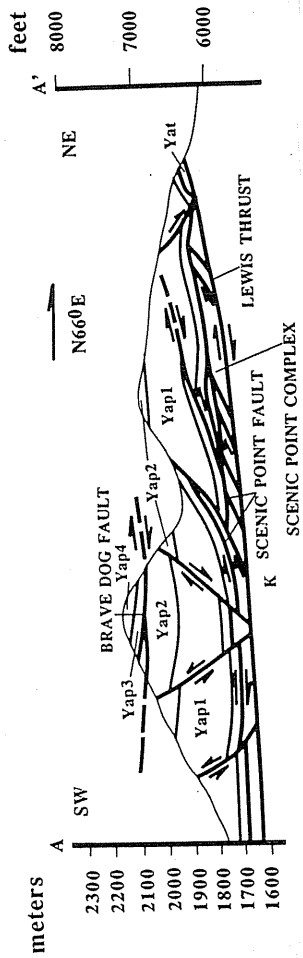


Fig. 5b

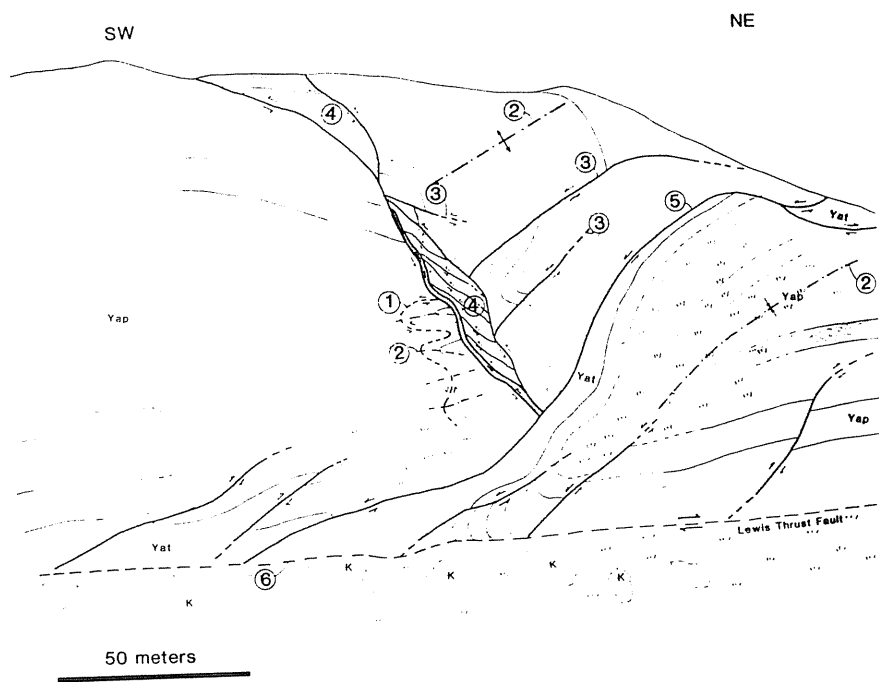


Fig. 6. View of the frontal zone from south and sketch of structures shown in the photo.

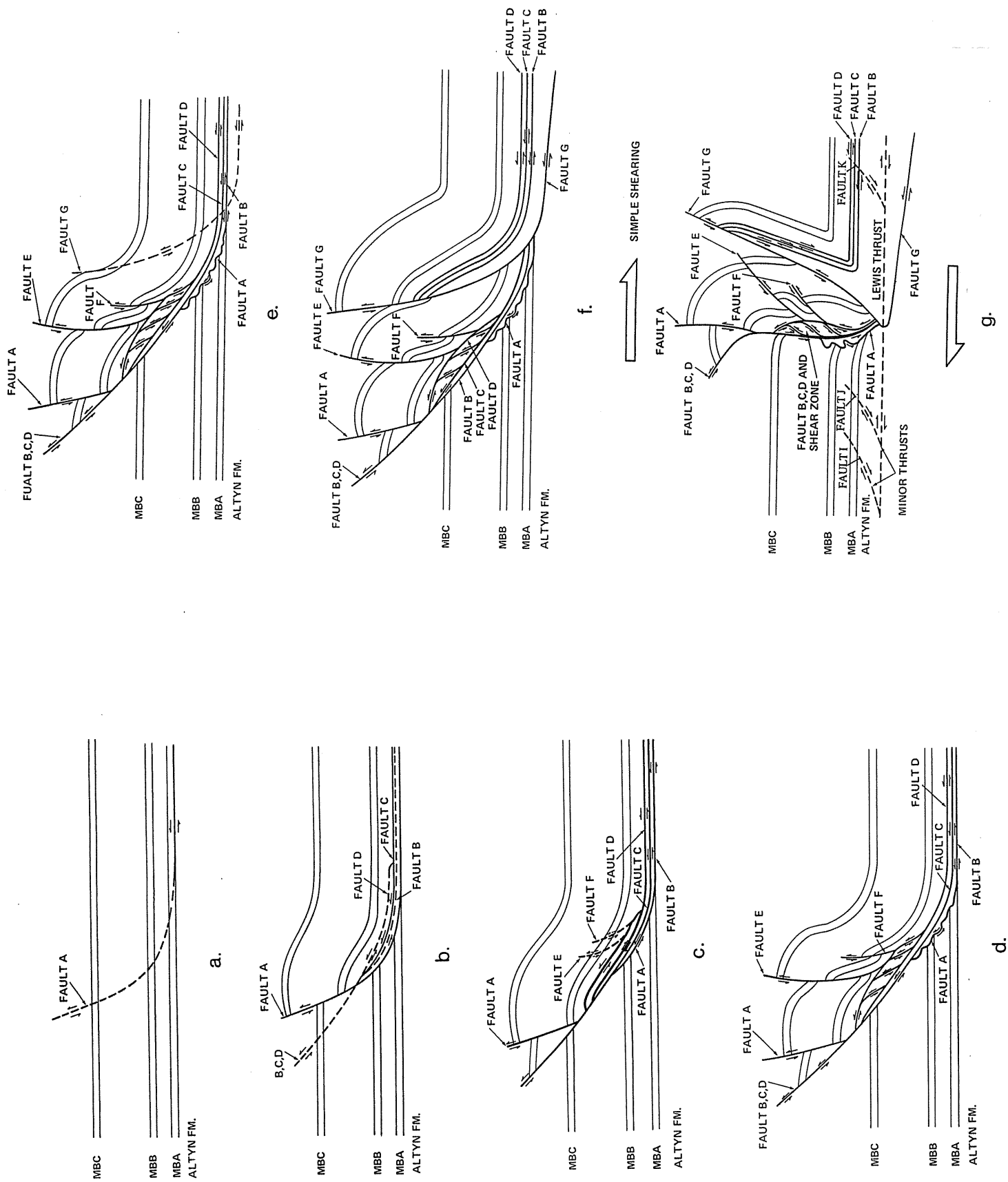
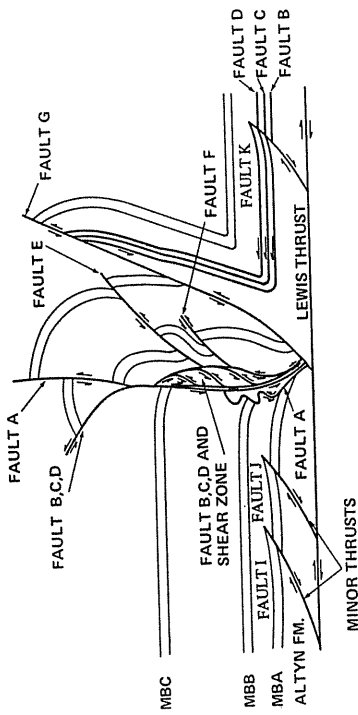
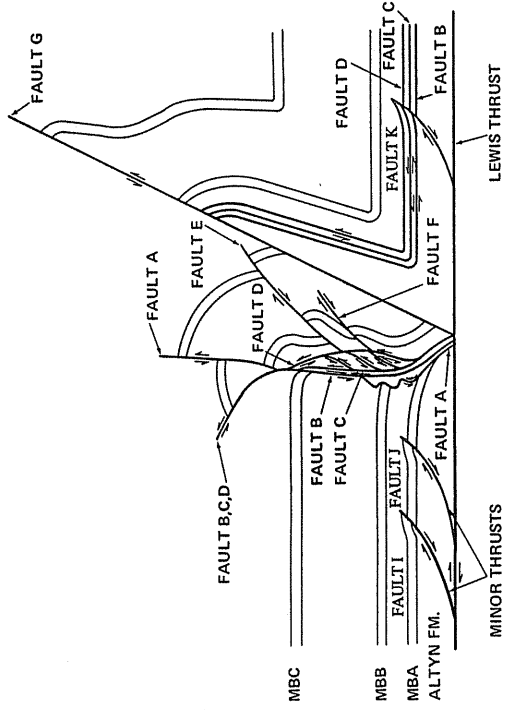
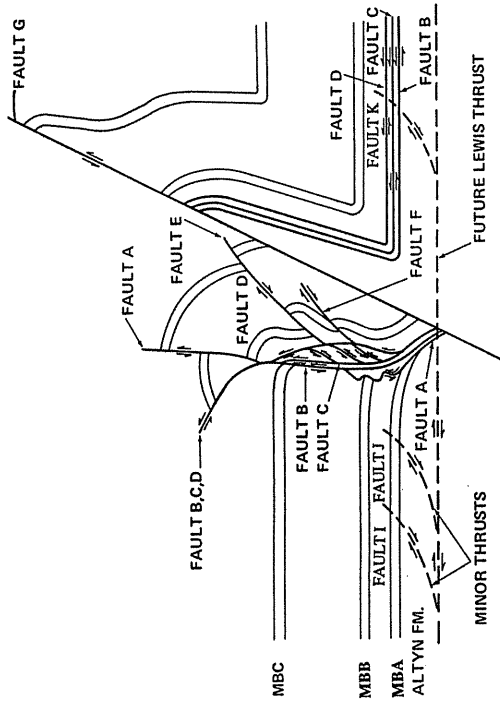
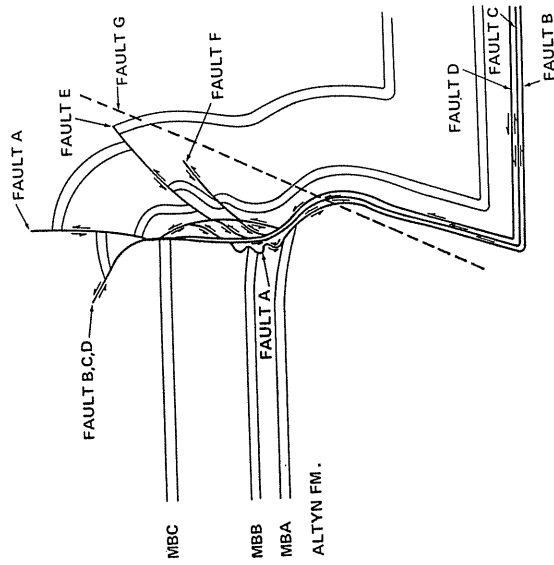


Fig. 7. Kinematic reconstruction of the frontal-zone deformation.



h.



i.

j.

k.

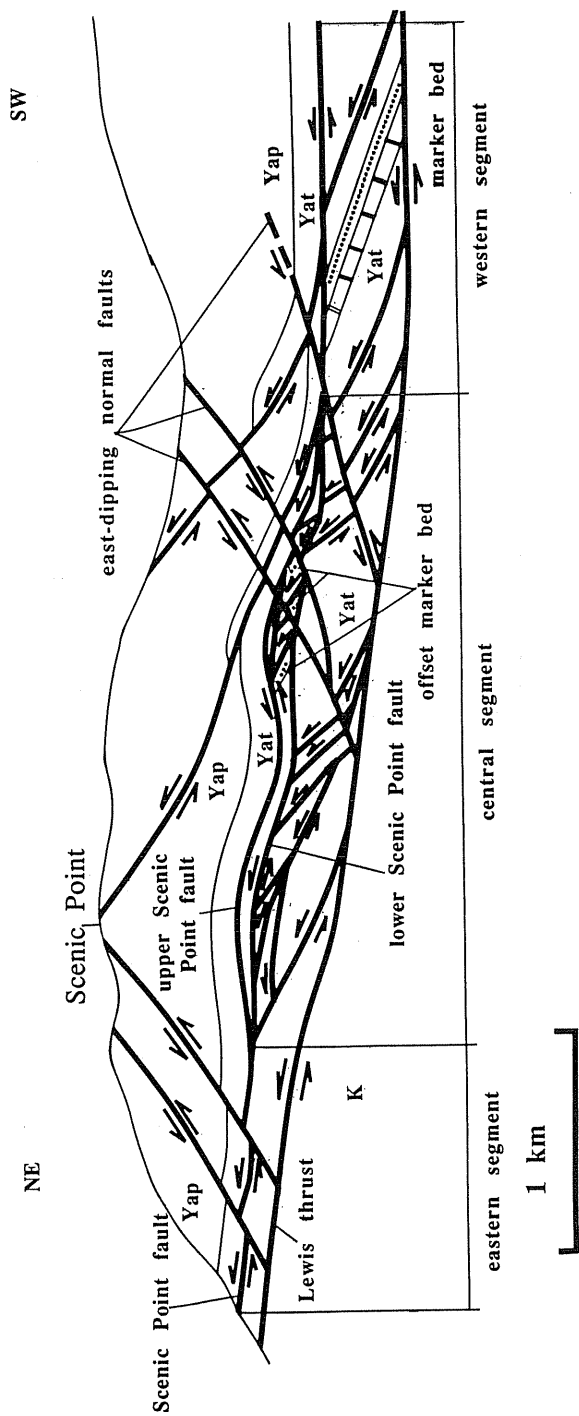


Fig. 8. Schematic cross section of Scenic Point structural complex based on field sketches and oblique photos. Yat, Allyn Formation; Yap, Appekunny Formation. Note that Scenic Point fault splits to upper and lower faults in its central segment, and lower Scenic Point fault displaced a quartz-arenite marker bed about 1 to 1.5 km to the east. Scenic Point fault truncates beds and imbricate thrusts in its hanging wall, indicating that it is an out-of-sequence fault. East-dipping normal faults cut Scenic Point complex.

Fig. 9a

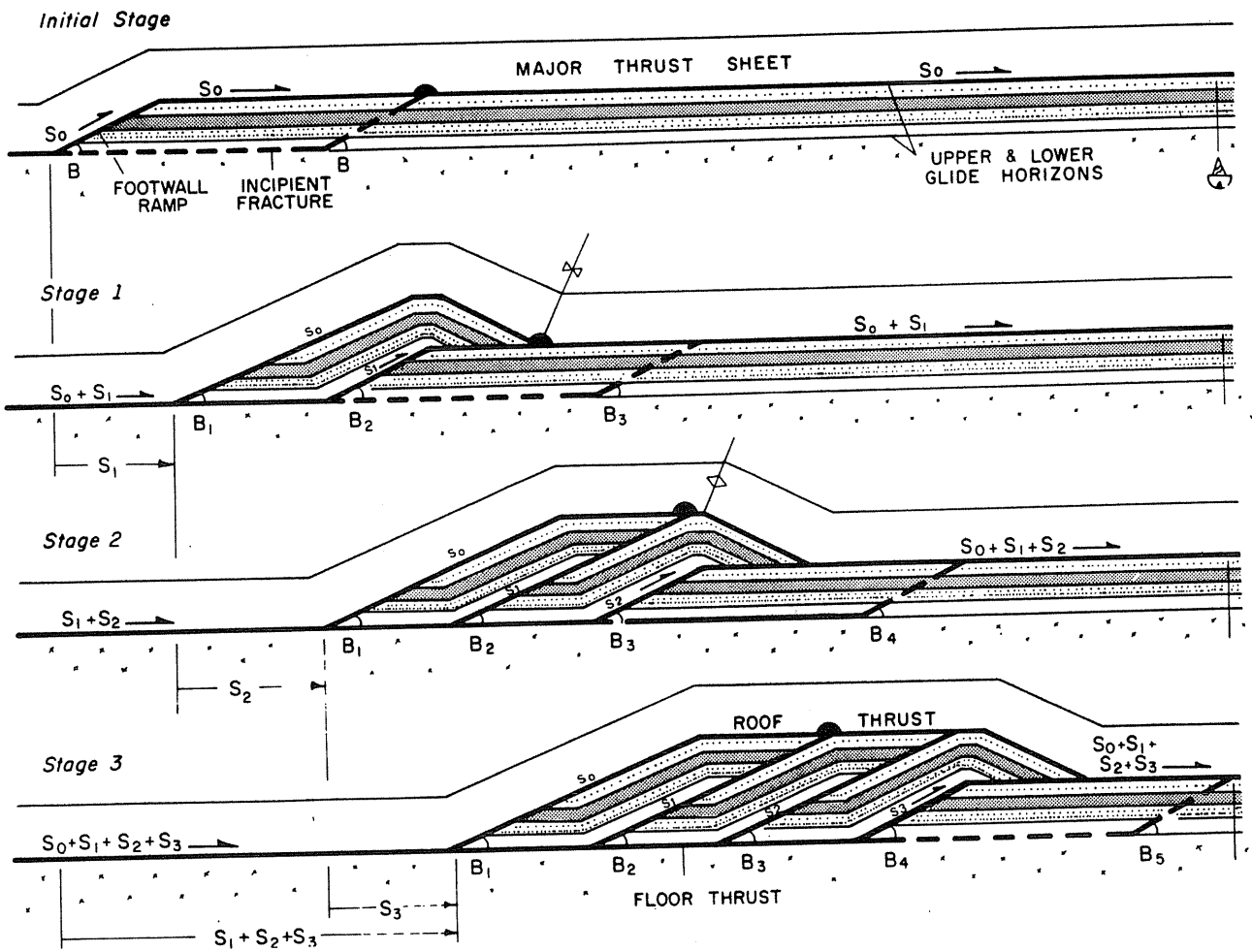


Fig. 9b

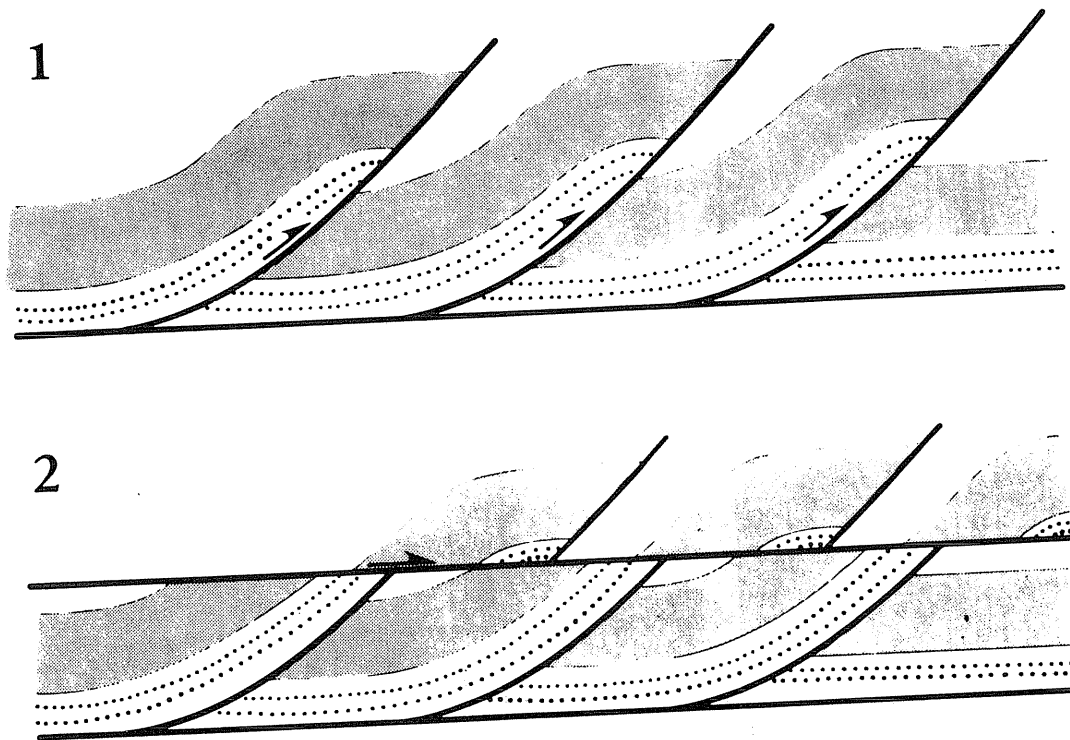


Fig. 9. Kinematic models for the formation of duplex systems after Boyer and Elliott (1982).

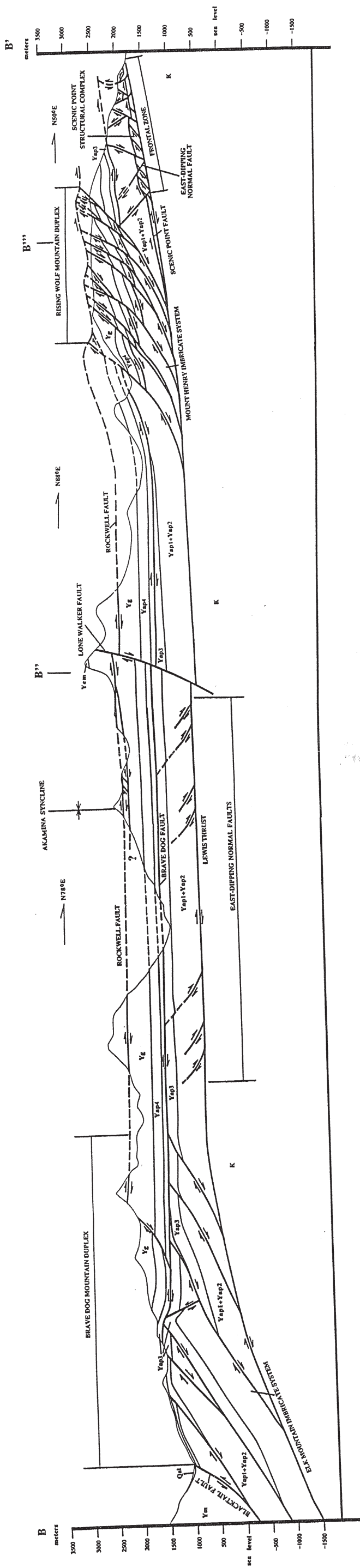
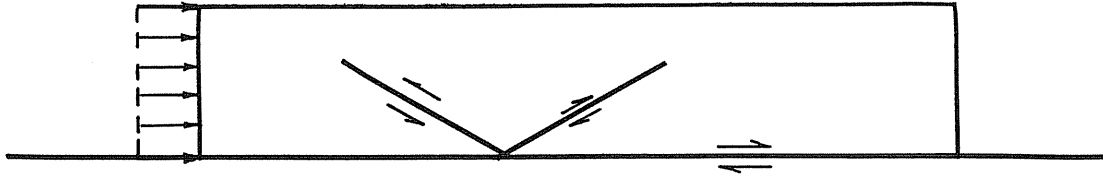


Fig. 10.

a. pure-shear deformation



b. simple-shear deformation

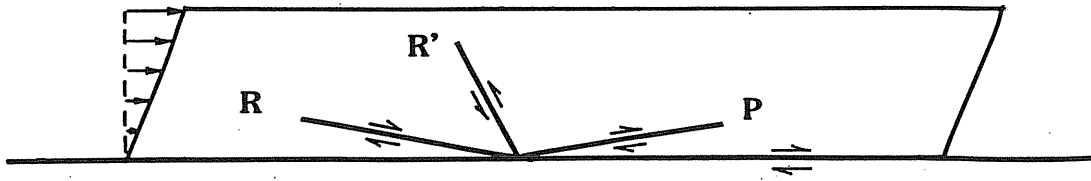


Fig. 11. Fault pattern predicted by pure-shear deformation and simple-shear deformation.

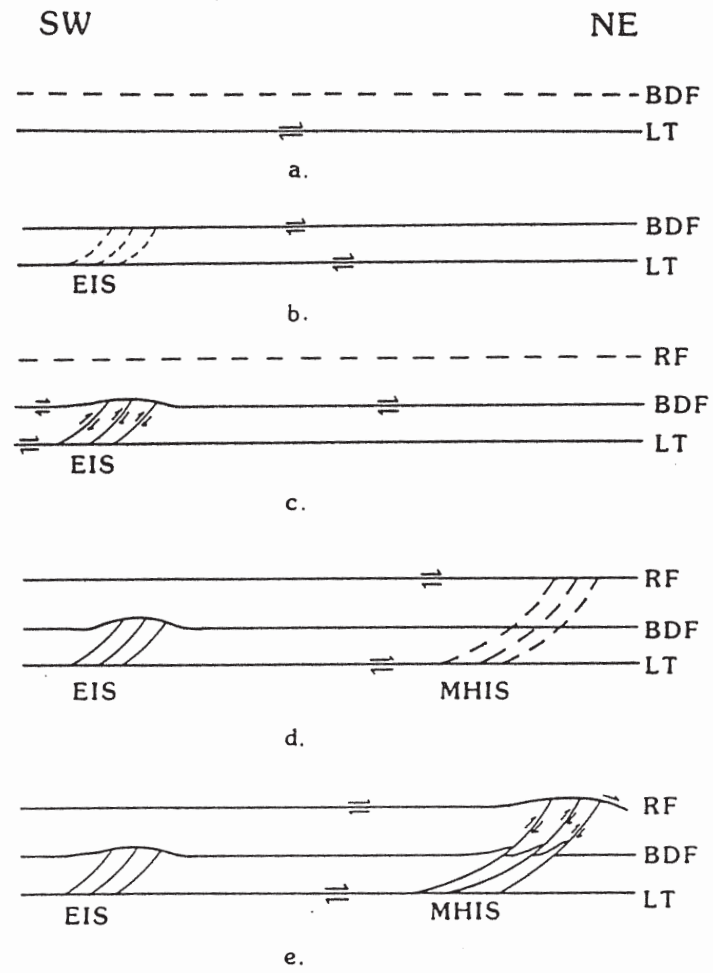
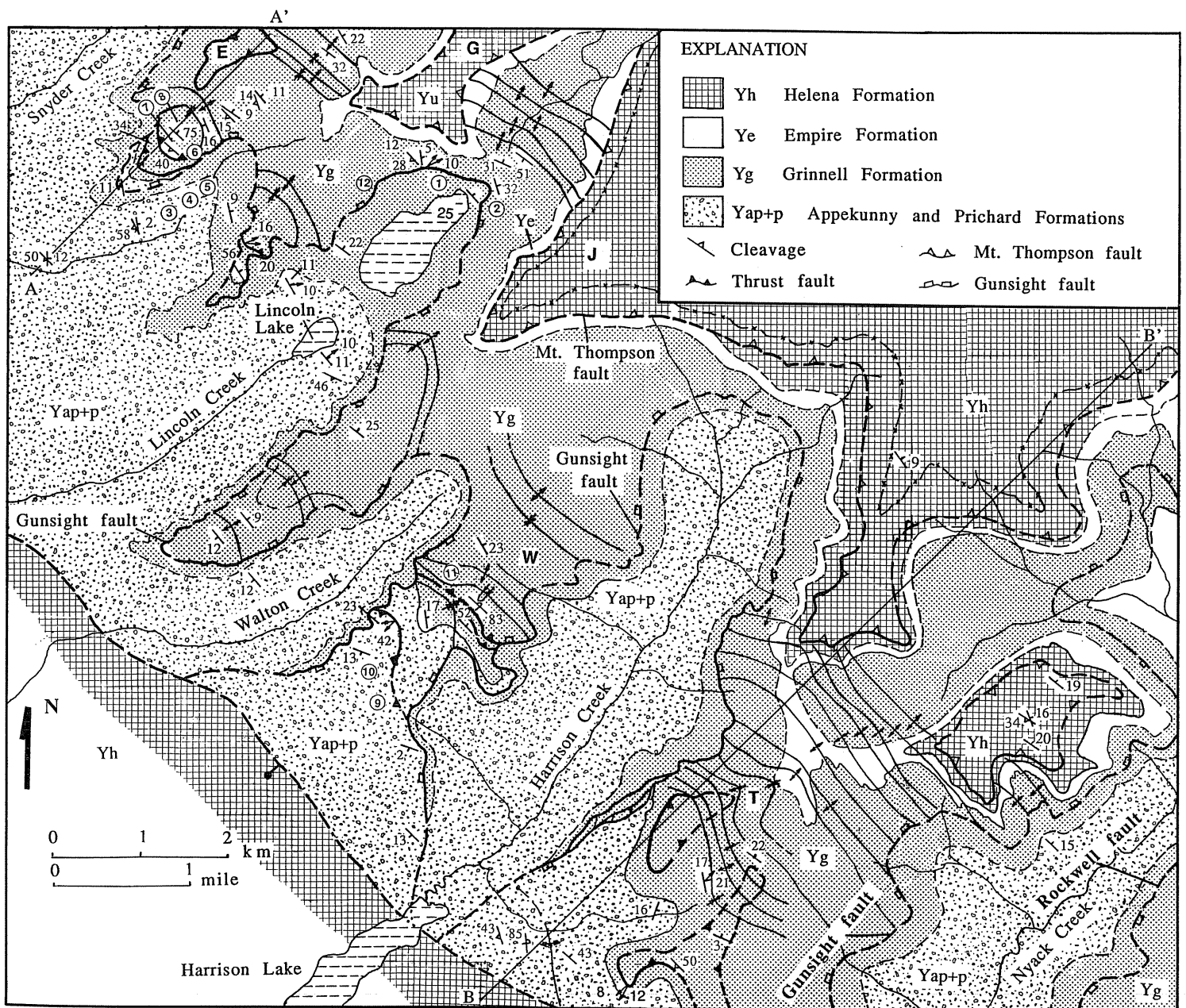


Fig. 12. Simple-shear model for the development of duplex systems, after Yin et al. (1989).

Fig. 14. Simplified geologic map of west-central Glacier Park and cross section BB'. E, Edwards Mountain; G, Gunsight Mountain; J, Jackson Mountain; W, Walton Mountain; T, Mount Thompson.



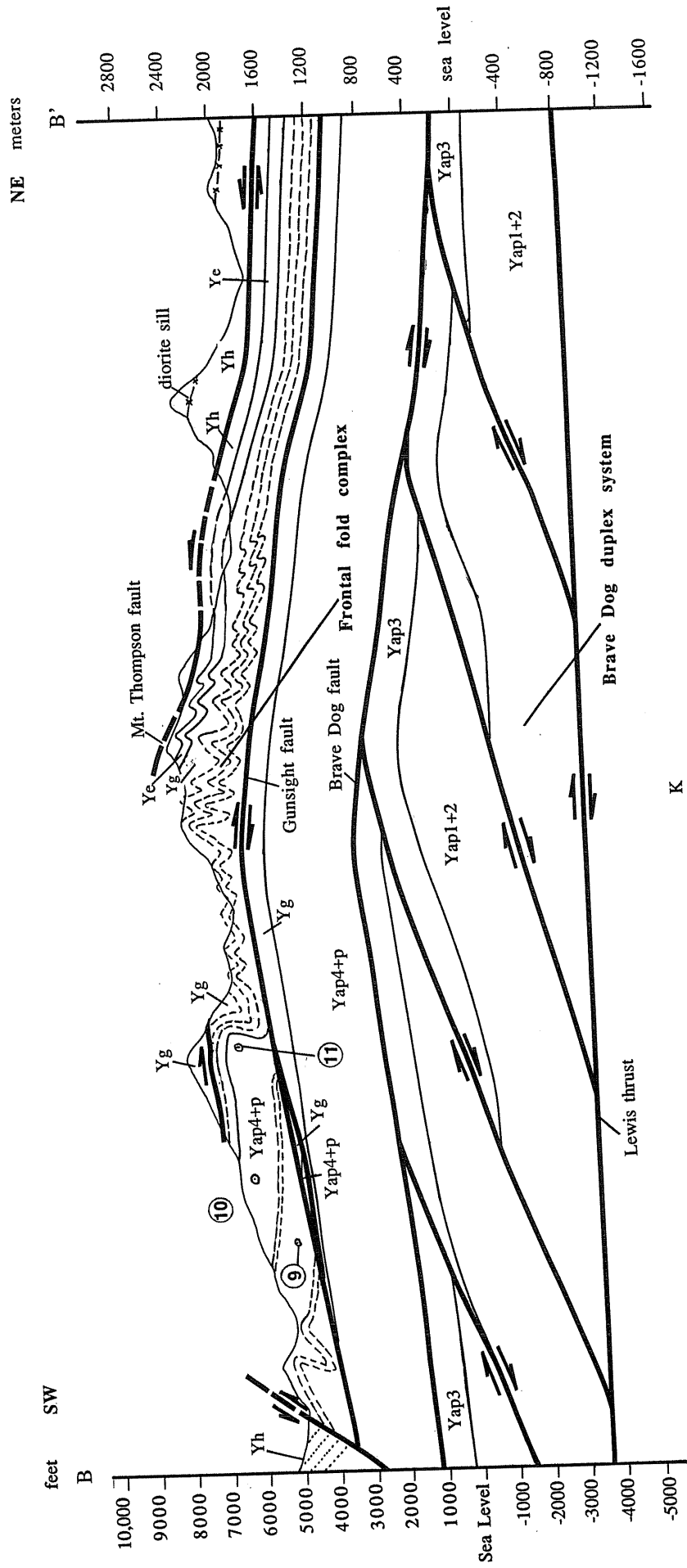


Fig. 14.

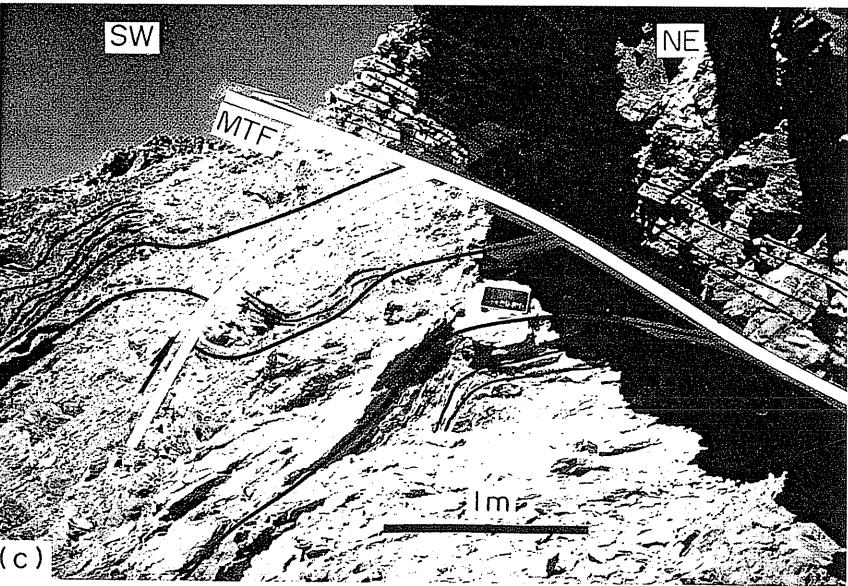
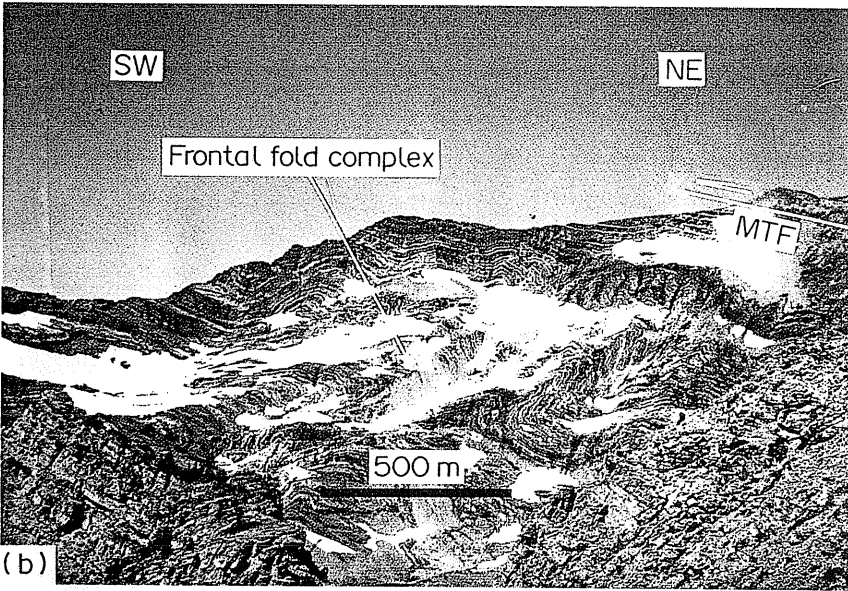
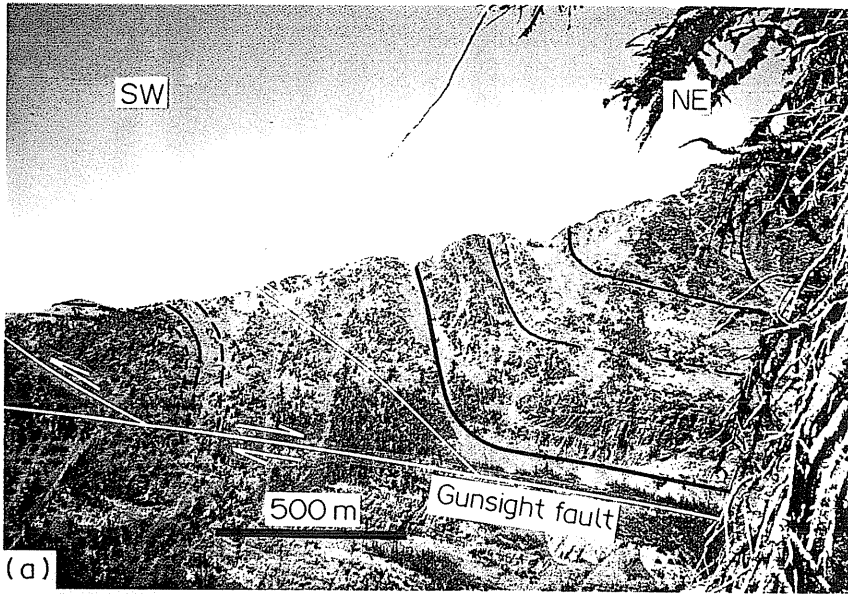


Fig. 15. a. A hanging-wall ramp and the fault-bend fold in the hanging wall of the Gunsight thrust at Walton Mountain viewed from the southeast.
 b. Frontal fold complex below the Mount Thompson roof fault on Mount Thompson, viewed from the south.
 c. Mount Thompson fault and west-verging folds immediately below on Mount Thompson, viewed from the south.

Evolution of footwall cut-off angle

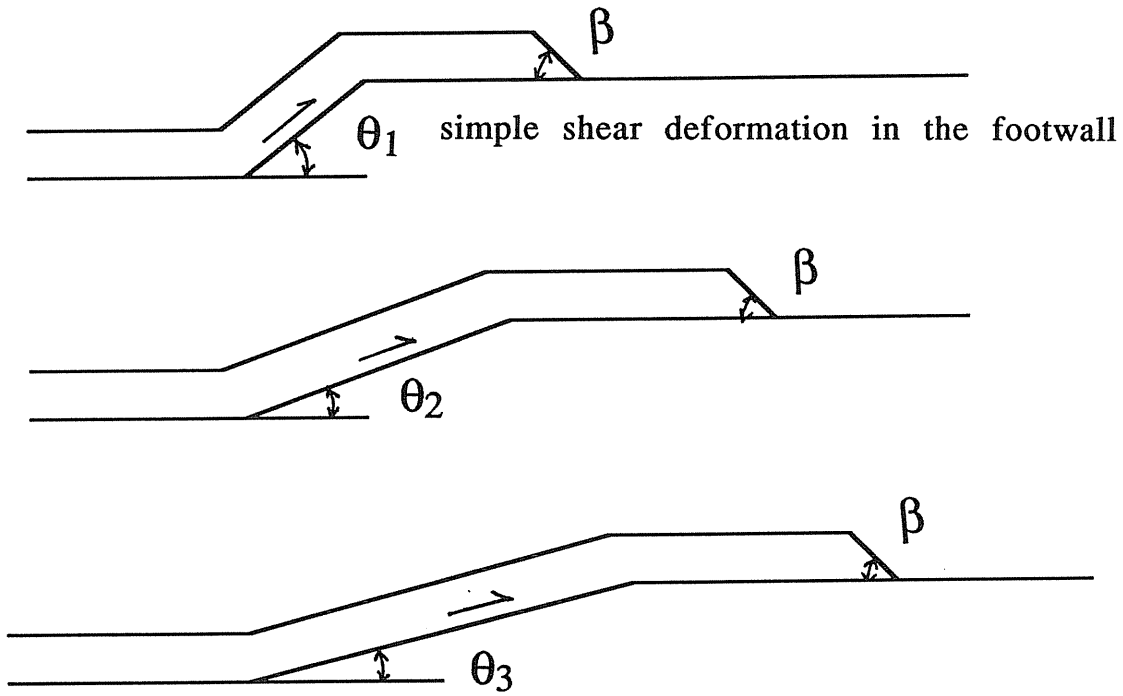


Fig. 16. Kinematic model for flattening of a thrust ramp due to bedding-parallel simple shear in its footwall.

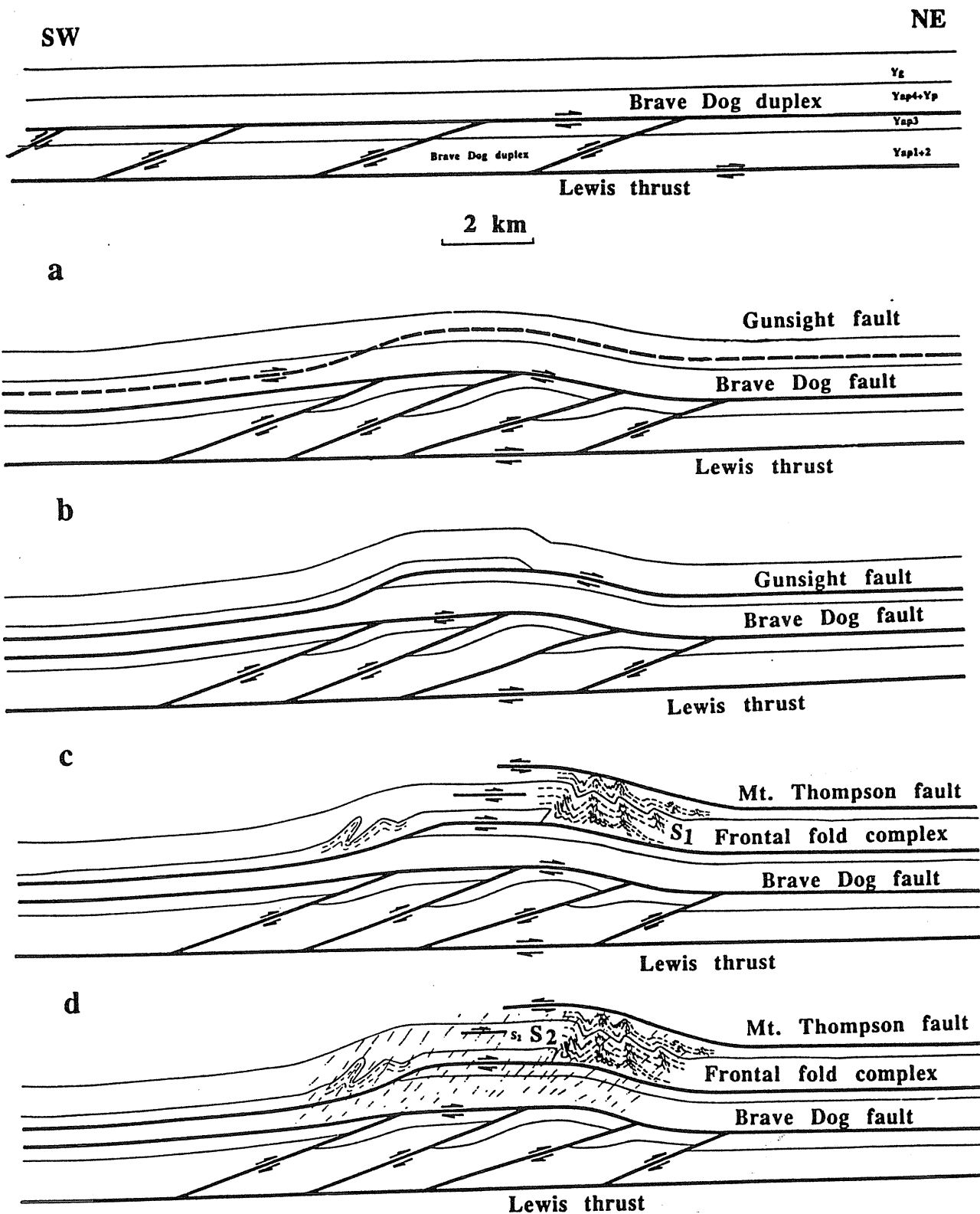


Fig. 17. Kinematic model for the development of fault-bend fold in west-central Glacier National Park, Montana.

a. Initiation and development of the Brave Dog duplex between Lewis thrust and Brave Dog fault. Yap1+2 for members 1 and 2 of the Appekunny Formation, Yap3 for member 3 of the Appekunny Formation, Yap4+p for member 4 of the Appekunny Formation and the Prichard Formation, and Yg for the Grinnell Formation.

b. Initiation of the Gunsight thrust above the antiformal Brave Dog fault.

c. Emplacement of the Gunsight thrust plate and development of the fault-bend fold as a consequence of motion along the Gunsight fault flat-ramp.

d. Formation of the hanging wall anticline and development of the frontal fold complex. Local top-to-the-west bedding-parallel shearing causing development of west-verging folds in the frontal fold complex and initiation of the W-directed Mount Thompson fault. NE-SW bedding-parallel shortening in the footwall and extension in the hanging wall as the anticlinal fault-bend fold develops further. Development of local east-dipping cleavage S₁ along the hinge zones with tightening of the west-verging folds in the frontal complex.

e. Development of west-dipping, regional cleavage S₂.

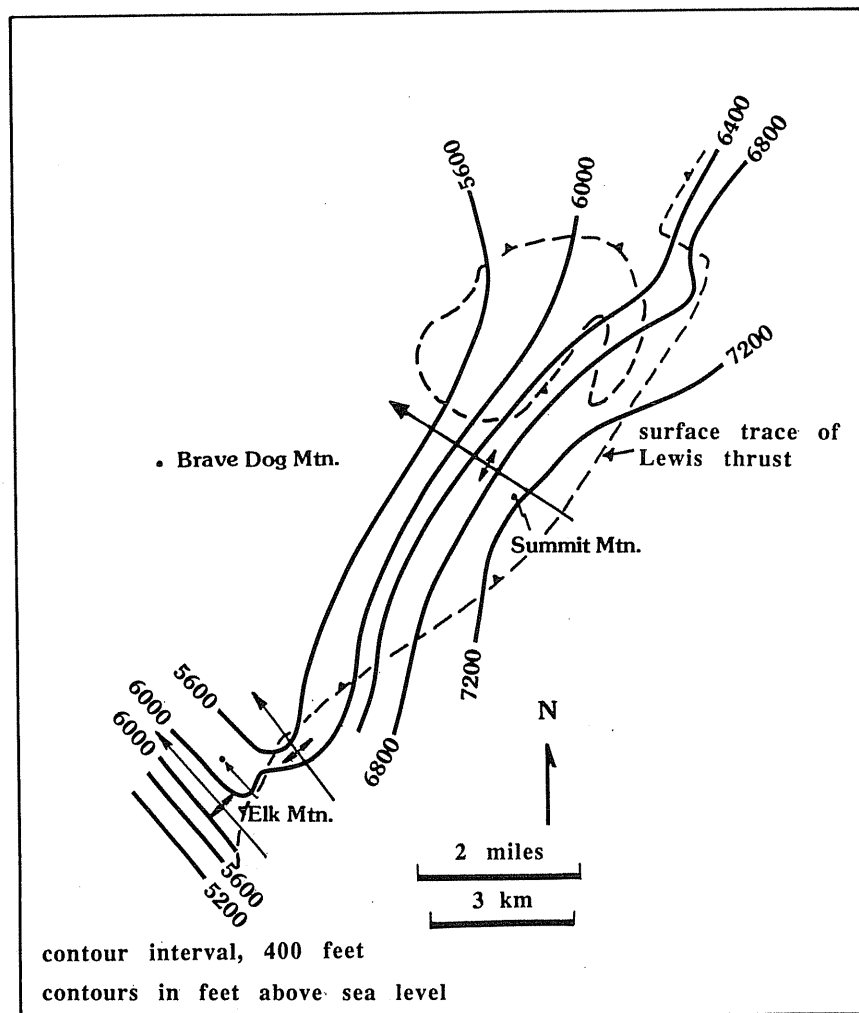


Fig. 18. Structural contour map of the Lewis thrust showing a gently northwest-dipping, oblique thrust ramp in southernmost part of study area. Dashed line, surface trace of the Lewis thrust; solid lines, contours of Lewis thrust surface. Contour interval, 400 feet; contours in feet above sea level. See Figure 2 for location. Construction of contours is based on surface trace of Lewis thrust and stratigraphic thicknesses of Altyn, Appekunny, and Grinnell Formations.

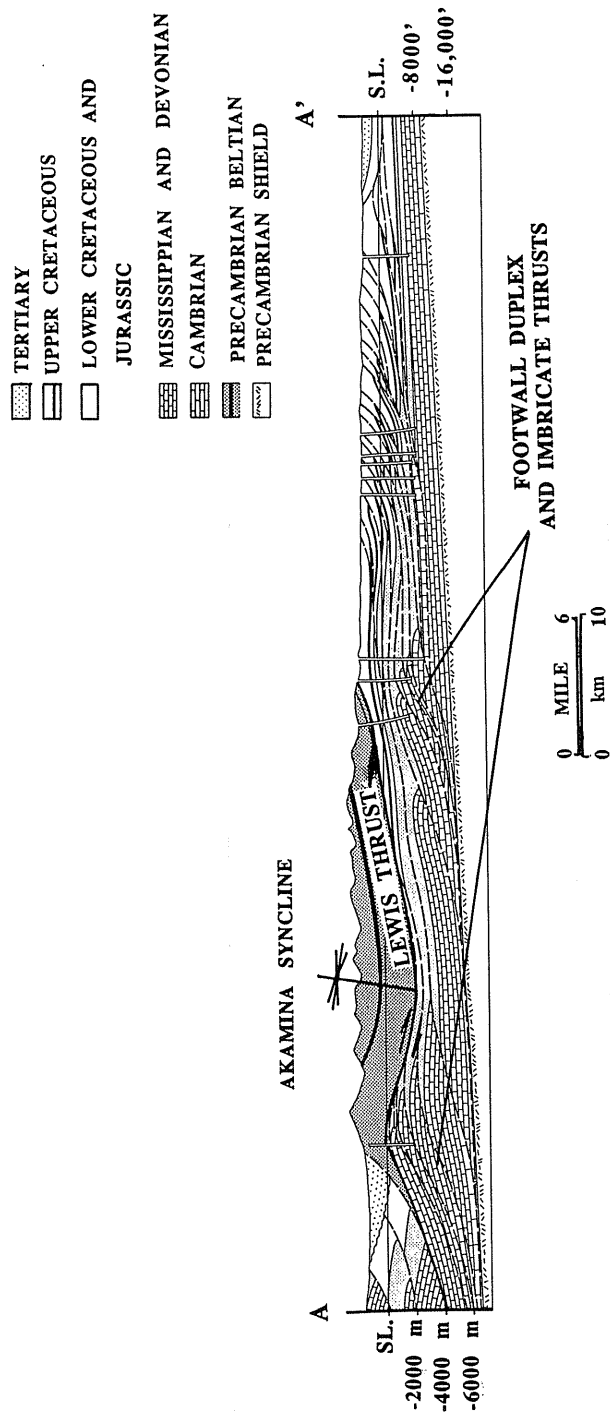


Fig. 19. Lewis thrust and underlying structures north of international border. Location of cross section AA' shown in Fig. 1, after Gordy et al. (1977). Note that Akamina syncline and Lewis thrust are concordantly folded. The syncline is interpreted to be related to duplex development and imbricate thrusting in footwall of Lewis thrust.

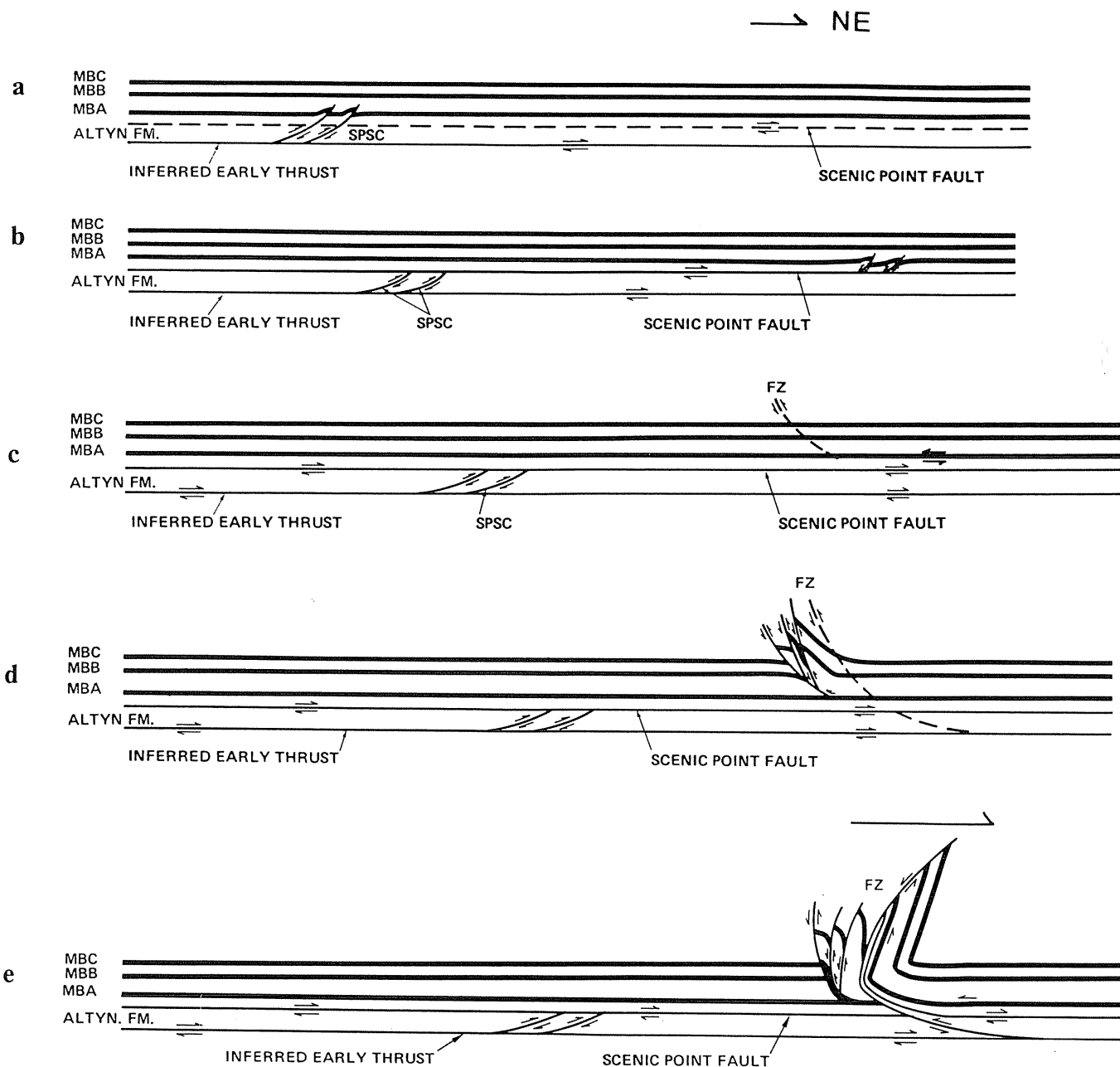
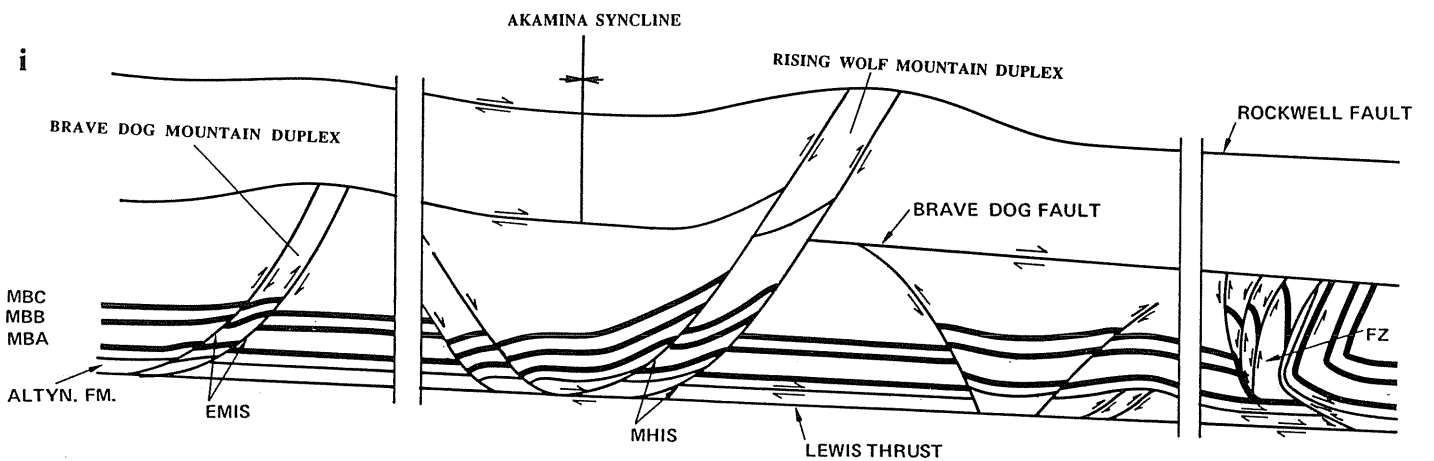
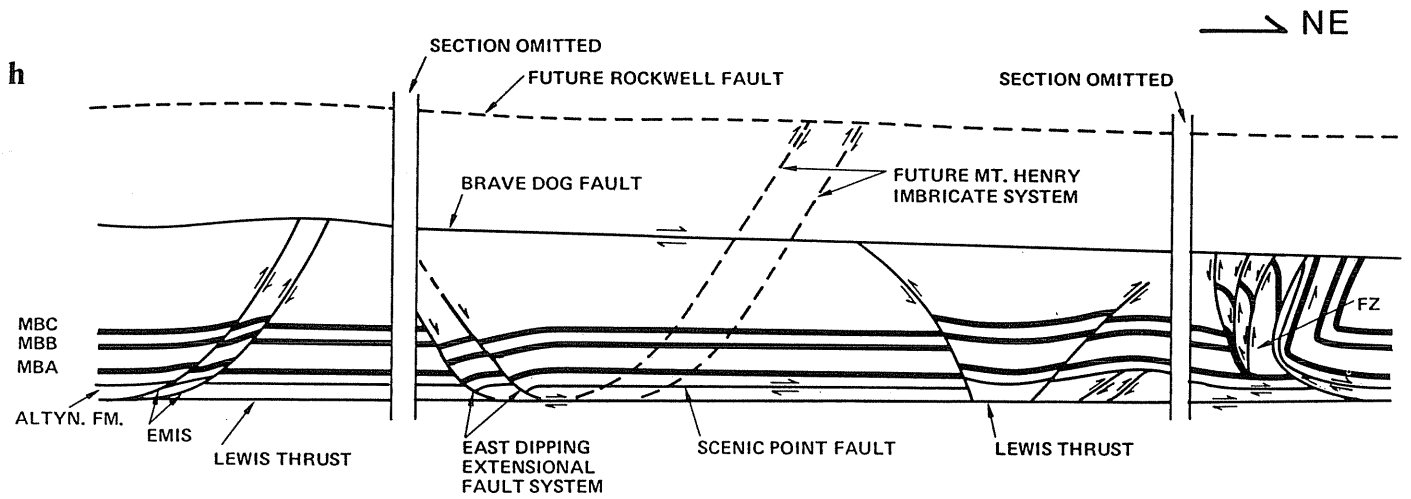
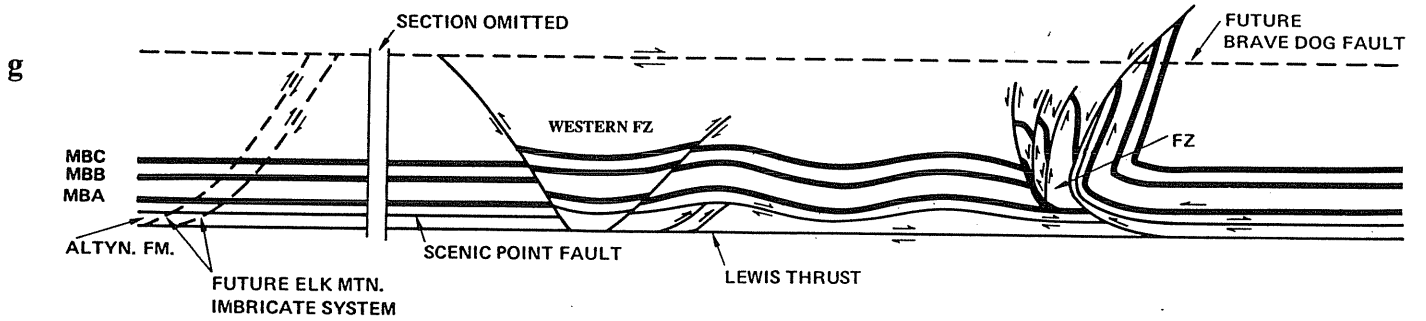
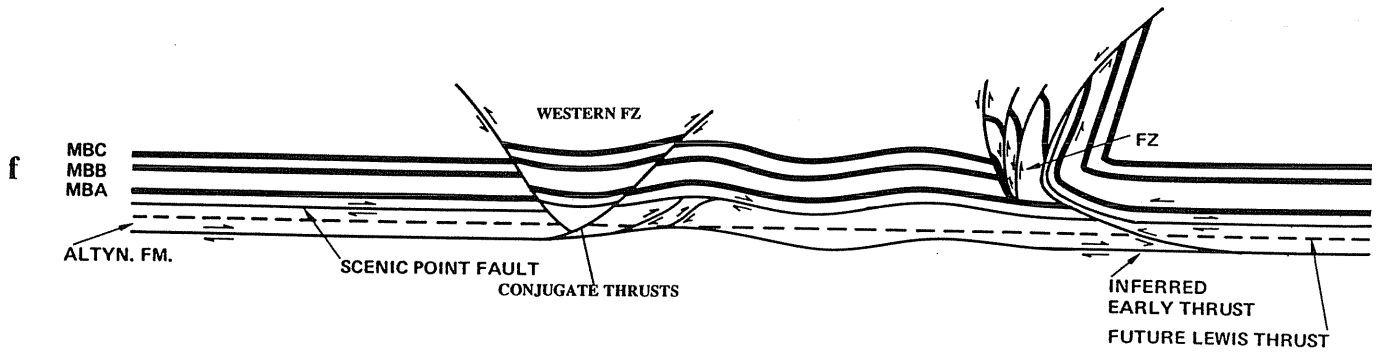


Fig. 20. Schematic sketch showing proposed deformation history of Lewis thrust system in southern Glacier National Park. MBA, MBB, and MBC are marker beds in Appekunny Formation. Marker bed A rests directly on top of Altyn Formation. EMIS, imbricate system in Brave Dog Mountain duplex; FZ, frontal zone; MHIS, imbricate system in Rising Wolf Mountain duplex; SPSC, Scenic Point structural complex.

- a. Development of imbricate thrusts in Scenic Point structural complex (SPSC). Imbricates branch off from an inferred early basal thrust. Initiation of Scenic Point fault.
- b. Imbricate thrusts in Scenic Point structural complex (SPSC) are offset by Scenic Point fault to the east. Scenic Point fault, thus, is an out-of-sequence thrust.
- c. Initiation of east-directed contraction faults in eastern frontal zone (FZ) along a decollement lying along the base of marker bed A (MBA).
- d. Further development of east-directed contraction faults in frontal zone along the inferred basal thrust. Younger faults in FZ cut older decollement and Scenic Point fault and developed along the inferred basal thrust.
- e. Rotation of structures in eastern frontal zone by an east-verging simple shear.
- f. Development of conjugate contraction faults in western frontal zone. Folding of inferred basal thrust and Scenic Point fault. Initiation of Lewis thrust.
- g. Truncation and displacement of Scenic Point structural complex and frontal zone by Lewis thrust. Initiation of Brave Dog fault and Elk Mountain imbricate system (EMIS) in Brave Dog Mountain duplex. Formation of the western limb of Akamina syncline.
- h. Development of Brave Dog Mountain duplex and warping of Brave Dog fault and bedding above it. Initiation and development of east-dipping normal faults between Brave Dog fault and Lewis thrust. Truncation of frontal zone by Brave Dog fault. Initiation of Rockwell fault and Mount Henry imbricate system (MHIS) of Rising Wolf Mountain duplex.
- i. Development of Rising Wolf Mountain duplex. Offset of Brave Dog fault by imbricate thrusts in Rising Wolf Mountain duplex. Formation of eastern limb of Akamina syncline.



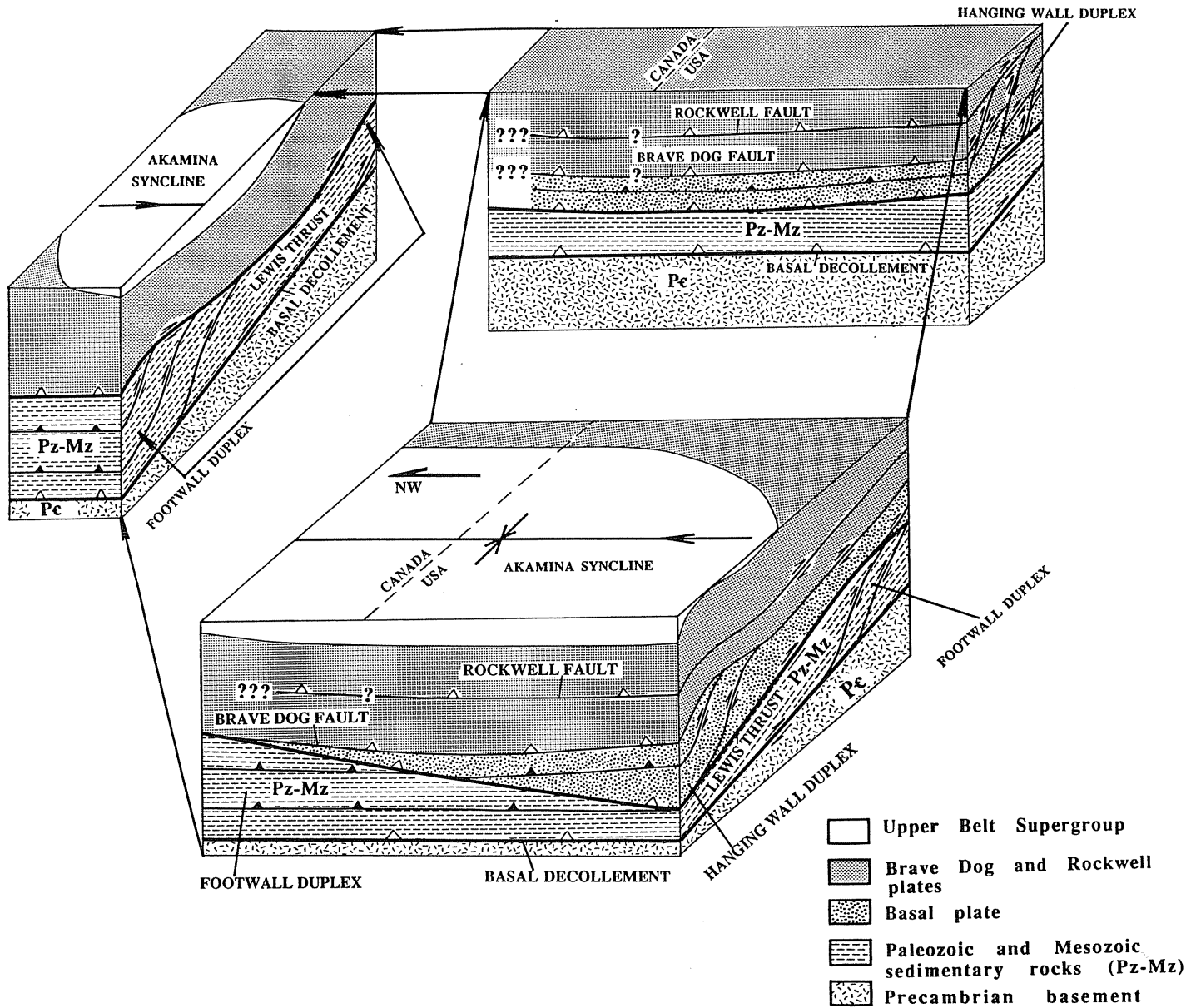


Fig. 21. Three-dimensional diagram showing structural relationship between Lewis thrust, Akamina syncline, duplexes in both hanging wall and footwall of Lewis thrust. Shortening accommodated by duplexes decreases in footwall and increases in hanging wall southward; Lewis thrust transferred NE-SW horizontal compression laterally from its footwall in Paleozoic and Mesozoic strata to its hanging wall in Proterozoic Belt strata.

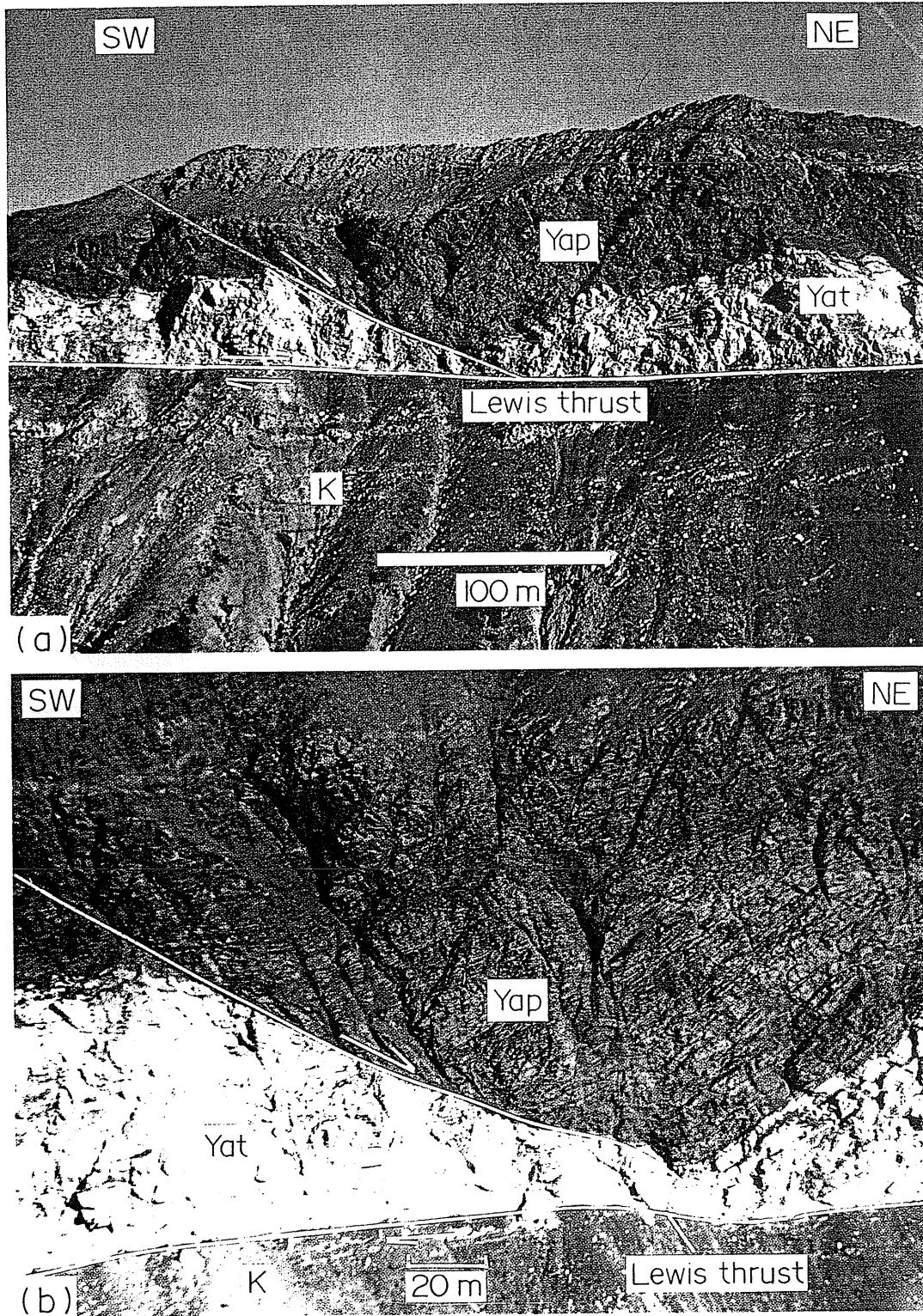


Fig. 22. (a) Oblique view of east-dipping normal fault above the Lewis thrust, Summit Mountain. Yap, Appekunny Formation; At, Altyn Formation; K, Cretaceous units. (b) Close-up of (a).

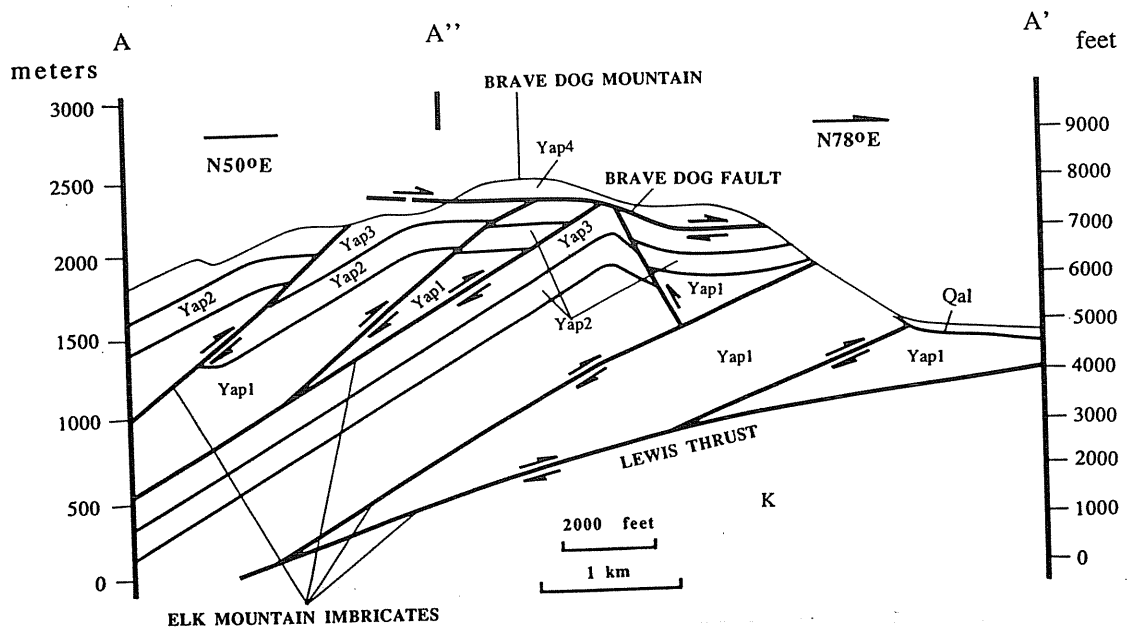
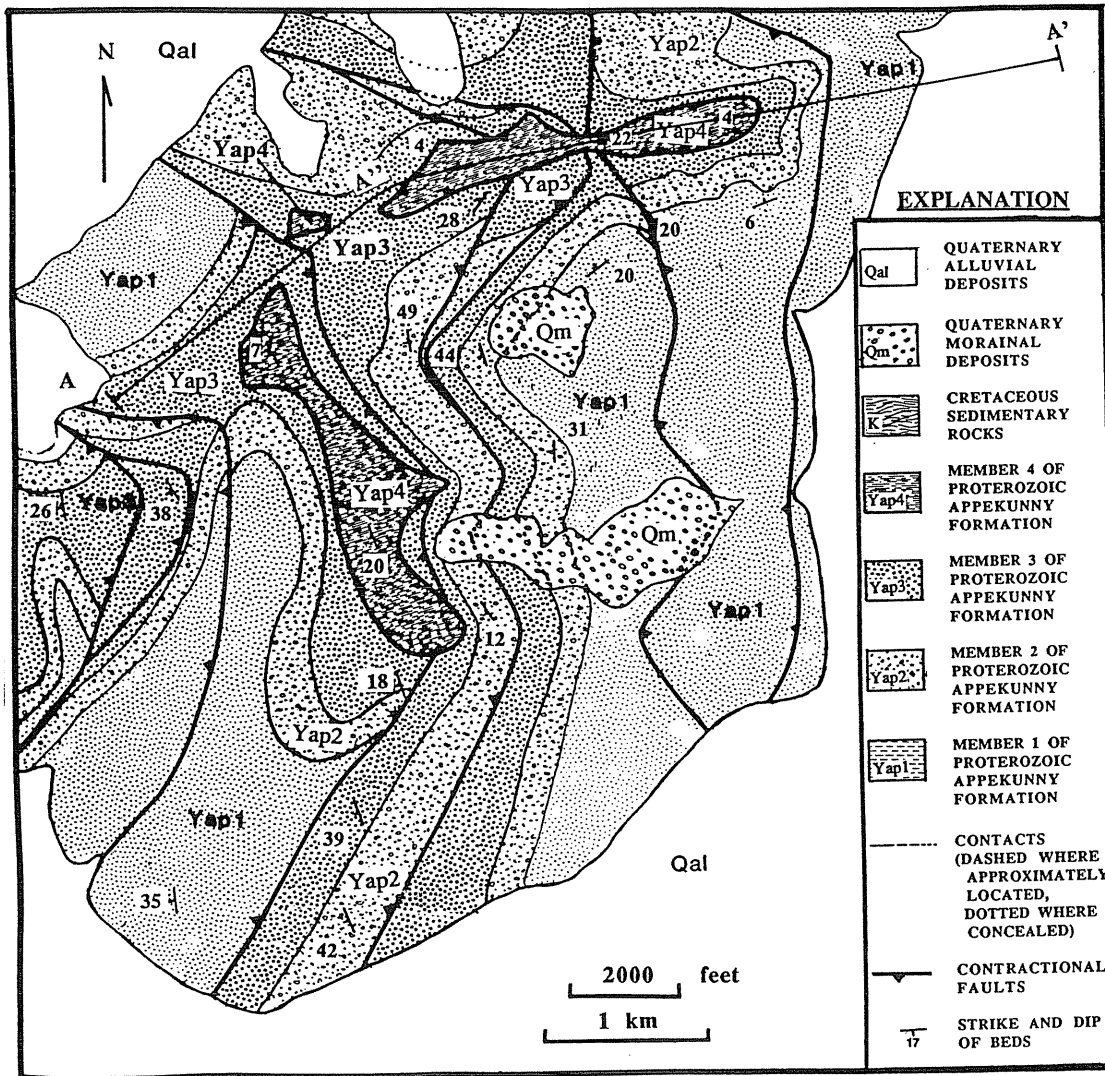


Fig. 23. a: Simplified geologic map of Brave Dog Mountain area after Kelty (1985). See Figure 2 for location. b: Geologic cross section through line AA'. Yap1-4, member 1 to 4 of Appekunny Formation. c: View of the Brave Dog duplex from south.



Fig. 23c

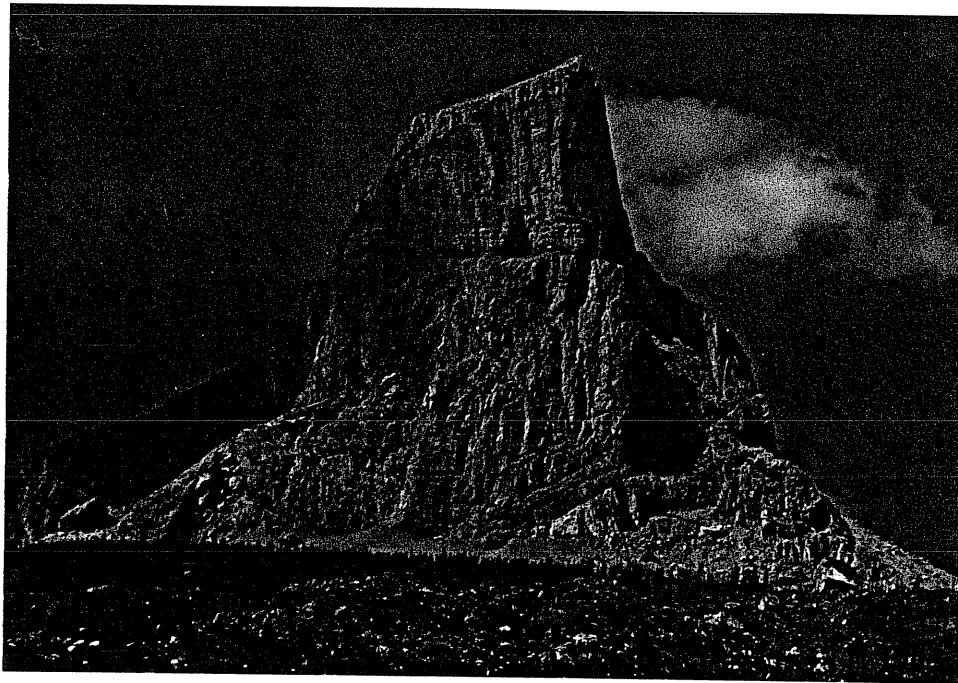


Fig. 24. View of the Chief Mountain duplex.

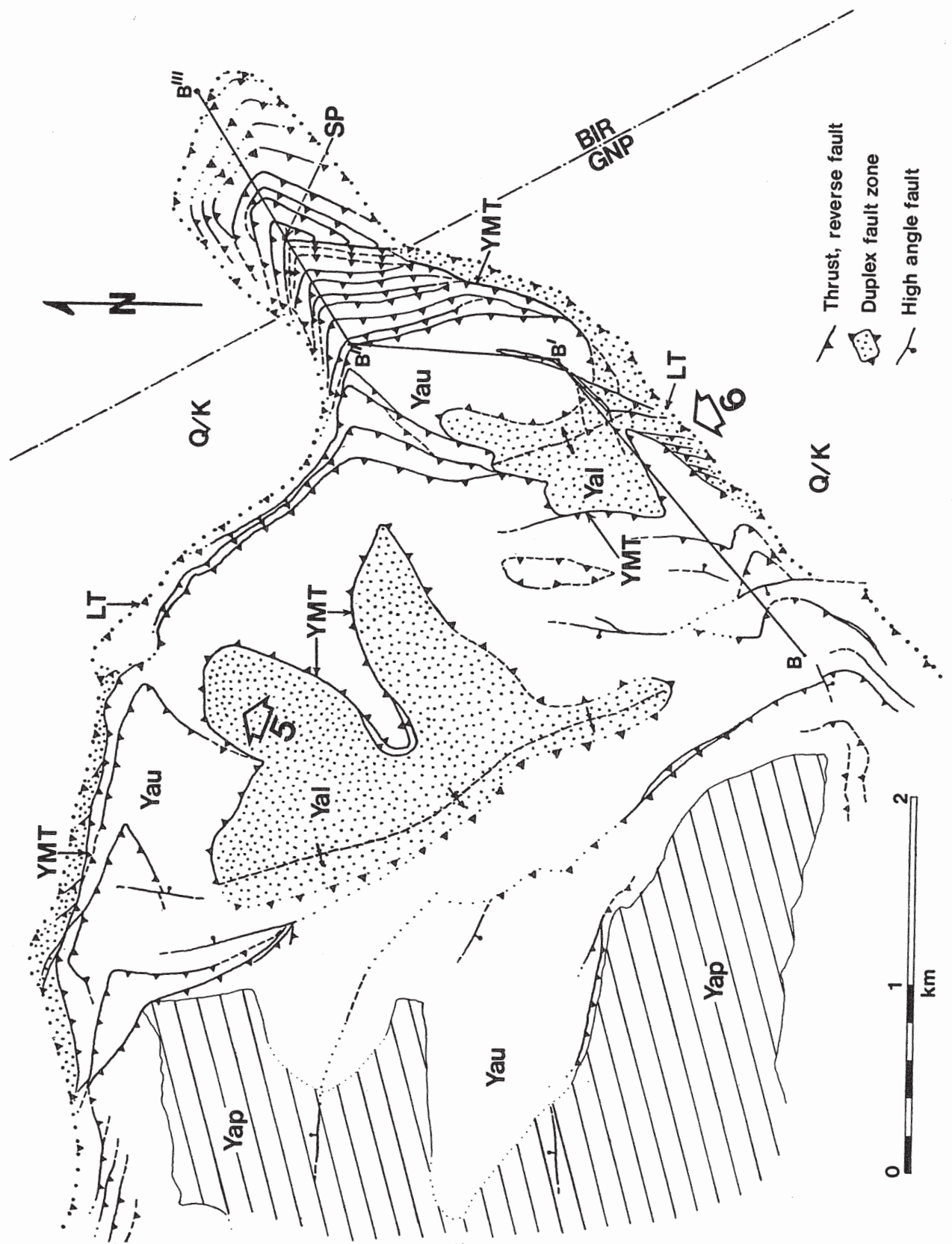


Fig. 25. Geologic map and cross-section of the Yellow Mountain duplex system.

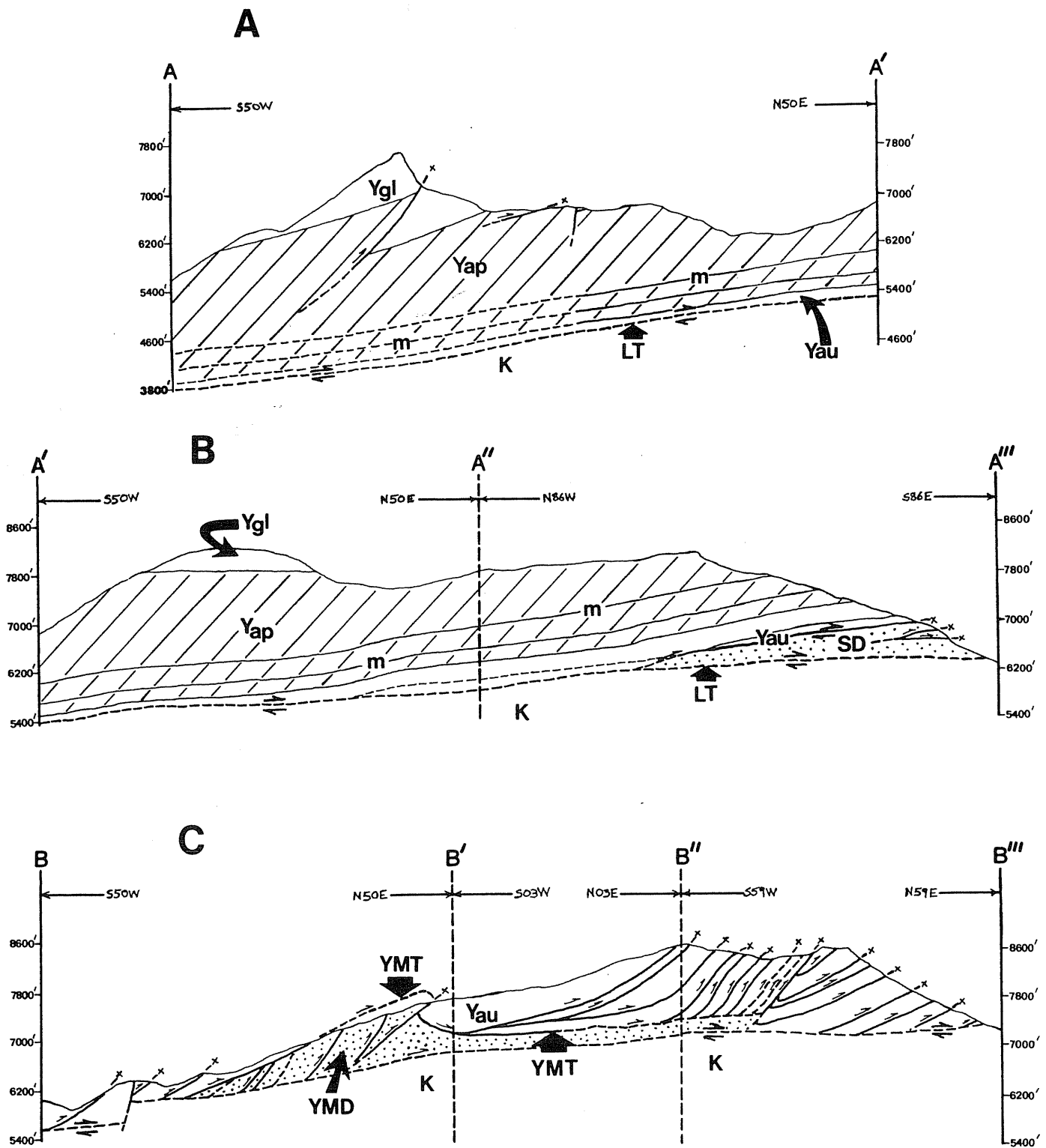


Fig. 25 b